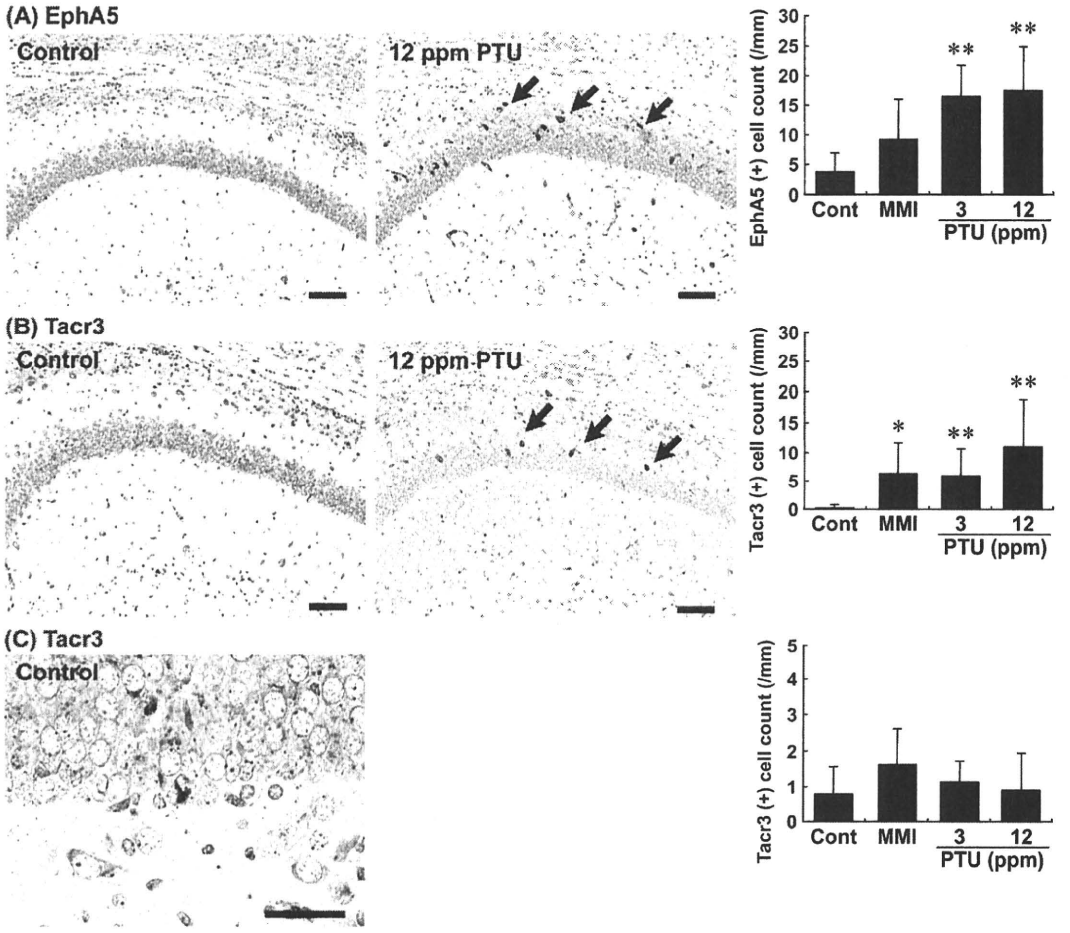

Fig. 3. Distribution of immunoreactive cells for EphA5 and Tacr3 in the hippocampal formation in rats at PND 20 after maternal exposure to anti-thyroid agents. (A) EphA5-immunoreactive cells with strong intensity located within the pyramidal cell layer and stratum oriens of the hippocampal CA1 region (arrows). Note the higher number of EphA5-positive cells in a case exposed to 12 ppm PTU (Right) as compared with the control animal (Left). Bar =100 μm. The graph shows the number of EphA5-positive cells/unit length (mm) of the CA1 region of the bilateral hemispheres. ** $P<0.01$ versus untreated controls (Student's *t*-test). (B) Tacr3-immunoreactive cells with strong intensity located within the pyramidal cell layer and stratum oriens of the hippocampal CA1 region (arrows). Note the higher number of Tacr3-positive cells in a case exposed to 12 ppm PTU (Right) as compared with the control animal (Left). Bar =100 μm. The graph shows the number of Tacr3-positive cells/unit length (mm) of the CA1 region of bilateral hemispheres. * $P<0.05$, ** $P<0.01$ versus untreated controls (Student's *t*-test). (C) Tacr3-immunoreactive cells located in the subgranular zone of the dentate gyrus. Bar =50 μm. The graph shows the number of Tacr3-positive cells/unit length (mm) of the subgranular zone of bilateral hemispheres. Abbreviations: EphA5, Ephrin type A receptor 5; MMI, 2-mercapto-1-methylimidazole; PTU, 6-propyl-2-thiouracil, Tacr3, Tachykinin receptor 3.

ampal formation: Immunohistochemical localization of EphA5 and Tacr3 in the hippocampal formation was examined at PND 20 and PNW 11.

On PND 20, EphA5 showed weak immunoreactivity in the pyramidal neurons throughout the hippocampal formation in the untreated controls. This immunoreactivity was unchanged by exposure to anti-thyroid agents. On the other hand, very sparse distribution of strongly immunoreactive cells for EphA5 was observed in the region of the CA1 pyramidal cell layer and stratum oriens in the untreated control animals, but immunoreactive cells were significantly increased showing scattered distribution by PTU at both 3 and 12 ppm (Fig. 3A). MMI-exposed animals also showed a small increase in the number of strongly positive cells with EphA5. Increased intensity in immunoreactivity of EphA5 was also observed in the gray matter consisting of neuropil at the stratum oriens of the CA1 region (Fig. 3A), and also in the molecular layer of the dentate gyrus at PND 20 after exposure to anti-thyroid agents, especially in PTU-exposed groups (data not shown).

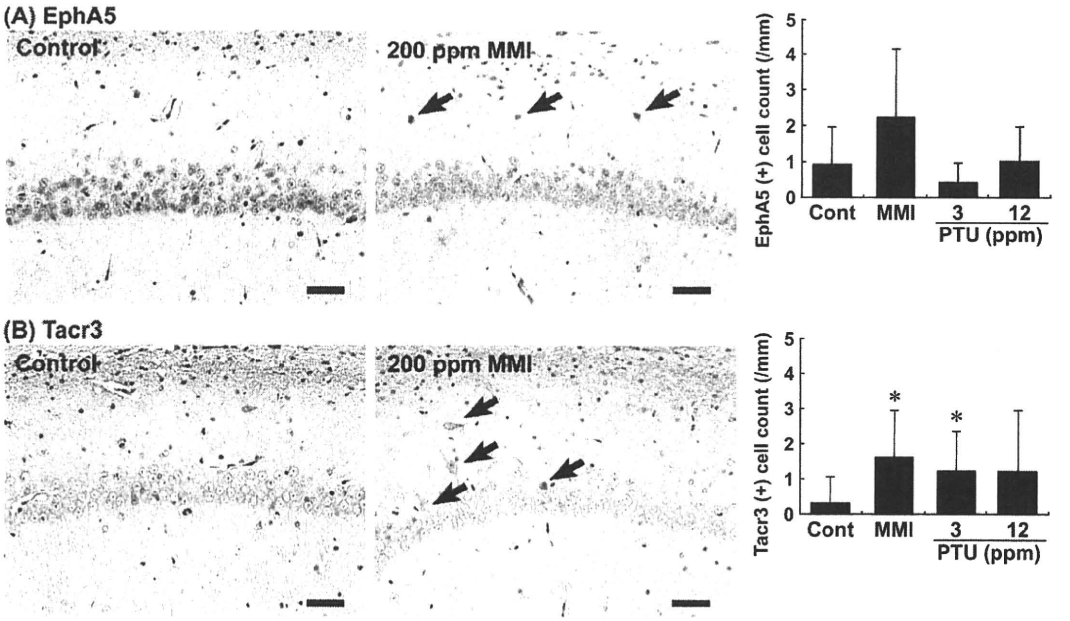

Fig. 4. Distribution of immunoreactive cells for EphA5 and Tacr3 in the hippocampal formation at PNW 11 of rats exposed maternally to anti-thyroid agents. (A) EphA5-immunoreactive cells with moderate staining intensity located within the pyramidal cell layer and stratum oriens of the hippocampal CA1 region. EphA5-positive cells in a case exposed to 200 ppm MMI (Right) as compared with the control animal (Left). The arrows show positive cells. Bar =50 μm. The graph shows the number of EphA5-positive cells/unit length (mm) of the CA1 region of the bilateral hemispheres. (B) Tacr3-immunoreactive cells with weak to moderate staining intensity located within the pyramidal cell layer and stratum oriens of the hippocampal CA1 region (arrows). Immunoreactivity is rather faint as compared with that observed at PND 20. Note the higher number of Tacr3-positive cells in a case exposed to 200 ppm MMI (Right) as compared with the control animal (Left). Bar =50 μm. The graph shows the number of Tacr3-positive cells/unit length (mm) of the CA1 region of bilateral hemispheres. * $P<0.05$ versus untreated controls (Student's t-test). Abbreviations: EphA5, Ephrin type A receptor 5; MMI, 2-mercapto-1-methylimidazole; PTU, 6-propyl-2-thiouracil; Tacr3, Tachykinin receptor 3.

With regards to Tacr3, the number of positive cells was increased with a scattered distribution showing strong intensity in the CA1 region similarly to that of EphA5 in the animals exposed to MMI or PTU on PND 20, but they were mostly absent in the untreated controls (Fig. 3B). Similarly, Tacr3-immunoreactive cells were sparse in the subgranular zone of the dentate gyrus in the MMI and PTU-exposed animals and in the untreated controls, but there were no differences in the number of positive cells as compared with the untreated controls (Fig. 3C). In addition, increased intensity in neuropil-immunoreactivity of Tacr3 was also observed in the strata oriens and radiatum of the CA1 region in all exposure groups of anti-thyroid agents (Fig. 3B).

On PNW 11, EphA5 showed weak immunoreactivity in the pyramidal neurons throughout the hippocampal formation in the untreated controls. This immunoreactivity was unchanged by exposure to anti-thyroid agents. EphA5-immunoreactive cells with moderate staining intensity were very sparsely observed in the region of the CA1 pyramidal cell layer and stratum oriens in the untreated control animals. There was no statistically significant increase in the number of these immunoreactive cells after exposure to PTU, while animals exposed to MMI showed a tendency for an increased number of immunoreactive cells (Fig. 4A). Increased neuropil-immunoreactivity of EphA5 as observed at PND 20 in exposure groups of anti-thyroid agents was mostly disappeared at PNW 11 (data not shown).

As well as at PND 20, Tacr3-immunoreactive cells were mostly absent in the untreated controls at PNW 11; however, a few immunoreactive cells with weak to moderate intensity were observed in the stratum oriens of the CA1 region in the animals exposed to anti-thyroid agents. There was a statistically significant difference in the animals treated with MMI or 3 ppm PTU compared with the untreated controls (Fig. 4B). Although the change was non-significant and lacked dose-dependence, 12 ppm PTU also showed an increasing tendency in the number of Tacr3-immunoreactive cells. In addition, increased neuropil-immunoreactivity of Tacr3 as observed at PND 20 in exposure groups of anti-thyroid agents was mostly disappeared at PNW 11 (data not shown).

DISCUSSION

In our recent study using rats [24], after maternal exposure to MMI or PTU, we detected typical hypothyroidism-related changes in the thyroid-related hormone levels, and hippocampal CA1 pyramidal neurons due to neuronal mismigration, as previously reported [8]. We also observed white matter changes, which seem to be due to impaired oligodendroglial development [6, 21]. To visualize molecules related to impaired neuronal development, microdissected CA1 region-specific global gene expression profiling was performed in the present study using the same animals that were used in our previous study. Two recently published studies have used microarrays to examine the expression profiles in the cerebral cortex and hippocampus of genes linked to developmental hypothyroidism caused by maternal PTU-exposure [7, 19]. In accordance with these studies, the genes that were significantly down-regulated in the present study included those that play roles in myelination, such as *Mobp* and myelin-associated glycoprotein, suggestive of the reflection of suppressed myelination by developmental hypothyroidism [21]. However, the genes that were found to be up-regulated on microdissected CA1 pyramidal cell layer, including *Efna5* and *Tacr3*, in the present study, have not been identified in previous studies. This difference may be related to the target tissues collected and the methods used, including microdissection of CA1 pyramidal cell layer from paraffin-embedded sections in the present study versus manual dissection of the cortical tissues from unfixed tissues in the previous studies.

EphA5 is a tyrosine kinase receptor that is almost exclusively expressed in the nervous system [15]. EphA5 and its ligand are important in mediating axon guidance, topographic projection, development, cell migration and the plasticity of limbic structures [15]. In addition, the transient expression of EphA5 during development is correlated with early neurogenesis and the migration of differentiated cells in the midbrain [3]. Thus, although expression of EphA5 was mostly weak in the euthyroid CA1 pyramidal neurons at PND 20, the increased number of EphA5-expressing cells with strong intensity in the CA1 region during developmental hypothyroidism in the present study reflects the neuronal mismigration caused by anti-thyroid agents. However, this increase was recovered after cessation of developmental hypothyroidism. Ephrins and their receptors are recently identified molecules and functional relationship between subfamily proteins is largely unknown; however, we, in the present study, found down-regulation of Epha7, another subfamily ephrin receptor, in all exposure groups of anti-thyroid agents (Table 1).

Tacr3, a member of the mammalian tachykinin peptide neurotransmitter/neuromodulator receptor family, is predominantly expressed in neurons in both the peripheral and central nervous systems, including the hippocampus [25]. There is increasing evidence of the role of Tacr3 on the survival and function of dopaminergic neurons. The survival of mesencephalic dopaminergic neurons during development largely depends on excitatory inputs, and tachykinins, through their receptors, are reported to play role in excitation [20]. On the other hand, senktide, a Tacr3 agonist, activates dopaminergic neurons to stimulate the release of dopamine and serotonin, and hyperlocomotion in gerbils [14]. Abnormal excitatory action of D_2-like receptor, one of the major subtypes of dopaminergic receptors, was observed on glutamatergic transmission in the CA1 synapses in the adult stage of rats after developmental hypothyroidism, suggesting a permanent disruption of synaptic integration in the CA1 neural networks [16]. While the role of Tacr3 in the hippocampal CA1 region during development is not clear, the increase in Tacr3-positive cells with strong intensity in this region during developmental hypothyroidism suggests a cell survival effect of tachykinin-3. Although the magnitude of the change was decreased, as compared with that at the end of the developmental hypothyroidism, the increased number of Tacr3-positive cells in the CA1 region of MMI and 3 ppm PTU-exposed animals may be an outcome of permanent disruption of synaptic integration, as described by Oh-Nishi *et al.* [16]. However, sparse distribution of Tacr3-positive cells may reflect that impairment sustained in a small population of aberrantly migrated neurons.

In conclusion, in this study, we have shown gene expression profiles showing altered expression in response to developmental hypothyroidism by analysis on microdissected hippocampal CA1 pyramidal cell layer in rats. Immunohistochemical analysis of the two candidate molecules revealed that developmental hypothyroidism until weaning is associated with the persistence of Tacr3-expressing neurons until the adult stage in the CA1 region, suggestive of the reflection of permanent disruption of synaptic integration. These findings probably reflect a mechanism to facilitate cell survival of aberrantly developed neurons due to mismigration.

ACKNOWLEDGMENT(S). We thank Miss Tomomi Morikawa for her technical assistance in conducting the animal study. We also thank Mrs. Shigeko Suzuki and Miss Ayako Kaneko for their technical assistance in preparing the histological specimens. This work was supported in part by Health and Labour Sciences Research Grants (Research on Risk of Chemical Substances) from the Ministry of Health, Labour and Welfare of Japan. All of the authors disclose that there are no conflicts of interest that could inappropriately influence the outcomes of the present study.

REFERENCES

1. Akaike, M., Kato, N., Ohno, H. and Kobayashi, T. 1991. Hyperactivity and spatial maze learning impairment of adult rats with temporary neonatal hypothyroidism. *Neurotoxicol. Teratol.* **13**: 317–322.
2. Comer, C. P. and Norton, S. 1982. Effects of perinatal methimazole exposure on a developmental test battery for neurobehavioral toxicity in rats. *Toxicol. Appl. Pharmacol.* **63**: 133–141.
3. Cooper, M. A., Crockett, D. P., Nowakowski, R. S., Gale, N. W. and Zhou, R. 2009. Distribution of EphA5 receptor protein

in the developing and adult mouse nervous system. *J. Comp. Neurol.* **514**: 310–328.

4. de Escobar, G. M., Obregón, M. J. and del Rey, F. E. 2007. Iodine deficiency and brain development in the first half of pregnancy. *Public Health Nutr.* **10**: 1554–1570.
5. Gerlai, R., Shinsky, N., Shih, A., Williams, P., Winer, J., Armanini, M., Cairns, B., Winslow, J., Gao, W. and Phillips, H. S. 1999. Regulation of learning by EphA receptors: a protein targeting study. *J. Neurosci.* **19**: 9538–9549.
6. Goodman, J. H. and Gilbert, M. E. 2007. Modest thyroid hormone insufficiency during development induces a cellular malformation in the corpus callosum: a model of cortical dysplasia. *Endocrinology* **148**: 2593–2597.
7. Kobayashi, K., Akune, H., Sumida, K., Saito, K., Yoshioka, T. and Tsuji, R. 2009. Perinatal exposure to PTU decreases expression of Arc, Homer 1, Egr 1 and Kcna 1 in the rat cerebral cortex and hippocampus. *Brain Res.* **1264**: 24–32.
8. Lavado-Autric, R., Ausó, E., García-Velasco, J. V., Arufe Mdel, C., Escobar del Rey, F., Berbel, P. and Morreale de Escobar, G. 2003. Early maternal hypothyroxinemia alters histogenesis and cerebral cortex cytoarchitecture of the progeny. *J. Clin. Invest.* **111**: 954–957.
9. Lee, K-Y., Shibutani, M., Inoue, K., Kuroiwa, K., U, M., Woo, G-H. and Hirose, M. 2006. Methacarn fixation—Effects of tissue processing and storage conditions on detection of mRNAs and proteins in paraffin-embedded tissues. *Anal. Biochem.* **351**: 36–43.
10. Masutomi, N., Shibutani, M., Takagi, H., Uneyama, C., Takahashi, N. and Hirose, M. 2003. Impact of dietary exposure to methoxychlor, genistein, or diisononyl phthalate during the perinatal period on the development of the rat endocrine/reproductive systems in later life. *Toxicology* **192**: 149–170.
11. Mileusnic, D., Lee, J. M., Magnuson, D. J., Hejna, M. J., Krause, J. E., Lorens, J. B. and Lorens, S. A. 1999. Neurokinin-3 receptor distribution in rat and human brain: an immunohistochemical study. *Neuroscience* **89**: 1269–1290.
12. Montero-Pedrazuela, A., Venero, C., Lavado-Autric, R., Fernández-Lamo, I., García-Verdugo, J. M., Bernal, J. and Guadaño-Ferraz, A. 2006. Modulation of adult hippocampal neurogenesis by thyroid hormones: implications in depressive-like behavior. *Mol. Psychiatry* **11**: 361–371.
13. Nakamura, R., Teshima, R., Hachisuka, A., Sato, Y., Takagi, K., Nakamura, R., Woo, G-H., Shibutani, M. and Sawada, J. 2007. Effects of developmental hypothyroidism induced by maternal administration of methimazole or propylthiouracil on the immune system of rats. *Int. Immunopharmacol.* **7**: 1630–1638.
14. Nordquist, R. E., Durkin, S., Jacquet, A. and Spooren, W. 2008. The tachykinin NK3 receptor agonist senktide induces locomotor activity in male Mongolian gerbils. *Eur. J. Pharmacol.* **600**: 87–92.
15. Numachi, Y., Yoshida, S., Yamashita, M., Fujiyama, K., Toda, S., Matsuoka, H., Kajii, Y. and Nishikawa, T. 2007. Altered EphA5 mRNA expression in rat brain with a single methamphetamine treatment. *Neurosci. Lett.* **424**: 116–121.
16. Oh-Nishi, A., Saji, M., Furudate, S. I. and Suzuki, N. 2005. Dopamine D_2-like receptor function is converted from excitatory to inhibitory by thyroxine in the developmental hippocampus. *J. Neuroendocrinol.* **17**: 836–845.
17. Olivieri, G. and Miescher, G. C. 1999. Immunohistochemical localization of EphA5 in the adult human central nervous system. *J. Histochem. Cytochem.* **47**: 855–861.
18. Porterfield, S. P. 2000. Thyroidal dysfunction and environmental chemicals—Potential impact on brain development. *Environ. Health Perspect.* **108**: 433–438.
19. Royland, J. E., Parker, J. S. and Gilbert, M. E. 2008. A genomic analysis of subclinical hypothyroidism in hippocampus and neocortex of the developing rat brain. *J. Neuroendocrinol.* **20**: 1319–1338.
20. Salthun-Lassalle, B., Traver, S., Hirsch, E. C. and Michel, P. P. 2005. Substance P, neurokinins A and B, and synthetic tachykinin peptides protect mesencephalic dopaminergic neurons in culture via an activity-dependent mechanism. *Mol. Pharmacol.* **68**: 1214–1224.
21. Schoonover, C. M., Seibel, M. M., Jolson, D. M., Stack, M. J., Rahman, R. J., Jones, S. A., Mariash, C. N. and Anderson, G. W. 2004 Thyroid hormone regulates oligodendrocyte accumulation in developing rat brain white matter tracts. *Endocrinology* **145**: 5013–5020.
22. Shibutani, M., Uneyama, C., Miyazaki, K., Toyoda, K. and Hirose, M. 2000. Methacarn fixation: a novel tool for analysis of gene expressions in paraffin-embedded tissue specimens. *Lab. Invest.* **80**: 199–208.
23. Shibutani, M., Lee, K-Y., Igarashi, K., Woo, G-H., Inoue, K., Nishimura, T. and Hirose, M. 2007. Hypothalamus region-specific global gene expression profiling in early stages of central endocrine disruption in rat neonates injected with estradiol benzoate or flutamide. *Dev. Neurobiol.* **67**: 253–269.
24. Shibutani, M., Woo, G-H., Fujimoto, H., Saegusa, Y., Takahashi, M., Inoue, K., Hirose, M. and Nishikawa, A. 2009. Assessment of developmental effects of hypothyroidism in rats from in utero and lactation exposure to anti-thyroid agents. *Reprod. Toxicol.* **28**: 297–307.
25. Smith, P. W. and Dawson, L. A. 2008. Neurokinin 3 (NK3) receptor modulators for the treatment of psychiatric disorders. *Recent Pat. CNS Drug Discov.* **3**: 1–15.
26. Takagi, H., Shibutani, M., Kato, N., Fujita, H., Lee, K-Y., Takigami, S., Mitsumori, K. and Hirose, M. 2004. Microdissected region-specific gene expression analysis with methacarn-fixed, paraffin-embedded tissues by real-time RT-PCR. *J. Histochem. Cytochem.* **52**: 903–913.
27. Uneyama, C., Shibutani, M., Masutomi, N., Takagi, H. and Hirose, M. 2002. Methacarn fixation for genomic DNA analysis in microdissected, paraffin-embedded tissue specimens. *J. Histochem. Cytochem.* **50**: 1237–1245.
28. Woo, G-H., Takahashi, M., Inoue, K., Fujimoto, H., Igarashi, K., Kanno, J., Hirose, M., Nishikawa, A. and Shibutani, M. 2009. Cellular distributions of molecules with altered expression specific to thyroid proliferative lesions developing in a rat thyroid carcinogenesis model. *Cancer Sci.* **100**: 617–625.

Reproductive Toxicology 29 (2010) 407–414

Contents lists available at ScienceDirect

Reproductive Toxicology

journal homepage: www.elsevier.com/locate/reprotox

Sustained production of Reelin-expressing interneurons in the hippocampal dentate hilus after developmental exposure to anti-thyroid agents in rats

Yukie Saegusa[a,b], Gye-Hyeong Woo[c], Hitoshi Fujimoto[c], Sayaka Kemmochi[a,b], Keisuke Shimamoto[a,b], Masao Hirose[c,d], Kunitoshi Mitsumori[a], Akiyoshi Nishikawa[c], Makoto Shibutani[a,c,*]

[a] Laboratory of Veterinary Pathology, Tokyo University of Agriculture and Technology, 3-5-8 Saiwai-cho, Fuchu-shi, Tokyo 183-8509, Japan
[b] Pathogenetic Veterinary Science, United Graduate School of Veterinary Sciences, Gifu University, 1-1 Yanagido, Gifu-shi, Gifu 501-1193, Japan
[c] Division of Pathology, National Institute of Health Sciences, 1-18-1 Kamiyoga, Setagaya-ku, Tokyo 158-8501, Japan
[d] Food Safety Commission, Akasaka Park Bld. 22nd F. 5-2-20 Akasaka, Minato-ku, Tokyo 100-8989, Japan

ARTICLE INFO

Article history:
Received 16 November 2009
Received in revised form 23 February 2010
Accepted 21 March 2010
Available online 27 March 2010

Keywords:
Developmental hypothyroidism
Impaired brain development
Migration
Neurogenesis
Dentate gyrus
Reelin
GABAergic interneuron

ABSTRACT

To detect molecular evidence reflecting a permanent disruption of neuronal development due to hypothyroidism, distribution of Reelin-producing cells that function in neuronal migration and positioning was analyzed in the hippocampal dentate hilus using rats. From gestation day 10, maternal rats were administered either 6-propyl-2-thiouracil (PTU) at 3 or 12 ppm (0.57 or 1.97 mg/kg body weight/day) or methimazole (MMI) at 200 ppm (27.2 mg/kg body weight/day) in the drinking water and male offspring were immunohistochemically examined at the end of exposure on weaning (postnatal day 20) and at the adult stage (11-week-old). Offspring with MMI and 12 ppm PTU displayed evidence of growth retardation lasting into the adult stage. On the other hand, all exposure groups showed a sustained increase in Reelin-expressing cells in the dentate hilus until the adult stage in parallel with Calbindin-D-28K-expressing cells at weaning and with glutamic acid decarboxylase 67-positive cells in the adult stage, confirming an increase in γ-aminobutyric acid (GABA)ergic interneurons. At the adult stage, NeuN-positive postmitotic mature neurons were also increased in the hilus in all exposure groups, however, the increased population of Reelin-producing cells at this stage was either weakly positive or negative for NeuN, indicative of immature neurons. At weaning, neuroblast-producing subgranular zone of the dentate gyrus showed increased apoptosis and decreased cell proliferation suggestive of impaired neurogenesis. The results suggest that sustained increases of immature GABAergic interneurons synthesizing Reelin in the hilus could be a signature of compensatory regulation for impaired neurogenesis and mismigration during the neuronal development as a hypothyroidism-related brain effect rather than that secondary to systemic growth retardation.

1. Introduction

Thyroid hormones are essential for normal fetal and neonatal brain development. They control neuronal and glial proliferation in definitive brain regions and regulate neural migration and differentiation [1–3]. In humans, maternal hypothyroxinemia, early in pregnancy, may have adverse effects on fetal brain development and importantly, even mild–moderate hypothyroxinemia may result in suboptimal neurodevelopment [4]. These results may increase the concern of impaired brain development by exposure to thyroid hormone-disrupting chemicals in the environment. Particularly, groups of persistent organic pollutants, such as organochlorine pesticides and polychlorinated biphenyls, have been shown to be ubiquitous environmental pollutants because of their great chemical stability and lipid solubility [5]. In addition to the variety of effects including immunologic, teratogenic, reproductive, carcinogenic, and neurological effects [6], many of these compounds are known to induce hypothyroidism [7].

Experimentally, developmental hypothyroidism leads to growth retardation, neurological defects and impaired performance on a variety of behavioral learning actions [8,9]. Rat offspring exposed maternally to anti-thyroid agents such as 6-propyl-2-thiouracil (PTU) show impaired brain development, with impaired neuronal migration and white matter hypoplasia involving limited axonal myelination and oligodendrocytic

Abbreviations: CA1, cornu ammonis 1; CA2, cornu ammonis 2; CA3, cornu ammonis 3; Calb-D-28K, Calbindin-D-28K; DH, dentate hilus; GABA, γ-aminobutyric acid; GAD67, glutamic acid decarboxylase 67; GD, gestation day; MMI, methimazole; NeuN, neuron-specific nuclear protein; PCNA, proliferating cell nuclear antigen; PND, postnatal day; PNW, postnatal week; PTU, 6-propyl-2-thiouracil; T_3, triiodothyronine; T_4, thyroxine; TSH, thyroid-stimulating hormone.

* Corresponding author at: Laboratory of Veterinary Pathology, Tokyo University of Agriculture and Technology, 3-5-8 Saiwai-cho, Fuchu-shi, Tokyo 183-8509, Japan. Tel.: +81 42 367 5874; fax: +81 42 367 5771.
E-mail address: mshibuta@cc.tuat.ac.jp (M. Shibutani).

0890-6238/$ – see front matter © 2010 Elsevier Inc. All rights reserved.
doi:10.1016/j.reprotox.2010.03.006

Table 1
Serum levels of thyroid-related hormones of the male offspring exposed to anti-thyroid agents during the period from the mid-gestation and lactation periods.

		Anti-thyroid agent in the drinking water		
	Untreated controls	200 ppm MMI	3 ppm PTU	12 ppm PTU
PND 20				
No. of offspring examined	10	9	10	9[a]
T_3 (ng/ml)	1.22 ± 0.10[b]	0.43 ± 0.19**	0.97 ± 0.31*	0.25 ± 0.03**
T_4 (μg/ml)	4.72 ± 0.84	1.06 ± 0.44**	1.86 ± 0.41**	1.06 ± 0.32**
TSH (ng/ml)	6.80 ± 2.11	35.33 ± 12.69**	27.38 ± 13.66**	27.69 ± 5.74**
PNW 11				
No. of offspring examined	10	10	10	6
T_3 (ng/ml)	1.02 ± 0.08	0.88 ± 0.09**	0.93 ± 0.11	0.84 ± 0.10**
T_4 (μg/ml)	5.11 ± 0.70	4.57 ± 1.04	5.12 ± 0.73	4.05 ± 0.71
TSH (ng/ml)	9.81 ± 3.16	9.41 ± 4.40	9.10 ± 3.25	7.75 ± 2.23

[a] $N = 7$ for measurement of T_3 and T_4 levels.
[b] Mean ± SD.
* Significantly different from the untreated controls (*$P < 0.05$).
** Significantly different from the untreated controls (**$P < 0.01$).

accumulation [2,10,11]. The outcome of this type of impaired brain development is permanent and is accompanied by apparent structural and functional abnormalities. However, it is still unclear whether the molecular aberrations remain in the retarded brain after maturation.

In the hippocampal formation, neuronal subpopulations are known to produce Reelin from embryonic period throughout adult life [12–16]. Reelin is a secreted extracellular matrix glycoprotein that plays a critical role in neuronal migration and positioning during brain development in the process regulated by thyroid hormone [13,17]. Also, in adults, it is suggested that Reelin released by γ-aminobutyric acid (GABA)ergic interneurons could regulate the migration and maturation of newborn granular cells in the dentate granular cell layer [18]. Altered Reelin signaling has been reported in the dentate gyrus of some neurological disease conditions, such as depression and epilepsy [18,19]. Within hippocampal formation, dentate gyrus is the unique structure that can continue neurogenesis during postnatal life and is a well-known target of developmental hypothyroidism [20].

In the present study, to detect a key molecular event reflecting permanent disruption of neuronal development due to exposure to xenobiotic chemicals that can interfere with thyroid hormone signaling, we examined temporal distribution change of Reelin-expressing cells in the dentate gyrus of rat offspring after developmental exposure to anti-thyroid agents. To distinguish chemical-specific expression changes from hypothyroidism-linked ones, two different anti-thyroid agents, methimazole (MMI) and PTU, were used, and dose-related responses were also examined with PTU.

Because of the similarities in the DNA binding domain of estrogen response element and thyroid hormone response element, crosstalk between the estrogen receptors and thyroid hormone receptors has been reported in previous studies [21,22]. Therefore, male offspring were selected for immunohistochemical analysis as well as measurement of serum thyroid-related hormones to avoid possible influence of estrogen in the present study.

2. Materials and methods

2.1. Chemicals and animals

Methimazole (2-mercapto-1-methylimidazole: MMI; CAS No. 60-56-0) and 6-propyl-2-thiouracil (PTU; CAS No. 51-52-5) were obtained from Sigma Chemical Co. (St. Louis, MO, USA). Pregnant Crj:CD®(SD)IGS rats were purchased from Charles River Japan Inc. (Yokohama, Japan) at gestation day (GD) 3 (appearance of vaginal plugs was designated as GD 0). Animals were housed individually in polycarbonate cages with wood chip bedding, maintained in an air-conditioned animal room (temperature: 24 ± 1 °C; relative humidity: 55 ± 5%) with a 12-h light/dark cycle and allowed *ad libitum* access to food and tap water. A soy-free diet (Oriental Yeast Co. Ltd., Tokyo, Japan) was chosen as the basal diet for the maternal animals to eliminate possible phytoestrogen effects [23], and water was given *ad libitum* throughout the experimental period including the 1-week acclimation period. On the other hand, all offspring consumed a regular CRF-1 basal diet (Oriental Yeast Co. Ltd.) and water *ad libitum* from PND 20 onwards (PND 0: the day of delivery). Although the formula is not open, CRF-1 contains soybean/alfalfa-derived proteins and oil including daidzin and genistin at concentrations of 87 and 102 ppm in diet according to the supplier's analysis, and coumestrol of less than 3 ppm based on the content of lucerne meal in the diet (supplier's comment). Soy-free diet was prepared based on the formulation of the NIH-07 open formula rodent diet, in which soybean meal and soy oil were replaced with ground corn, ground wheat, wheat middlings and corn oil. Values for phytoestrogens in this diet were below the detection limit (0.5 ppm), except for coumestrol with 3 ppm. Estrogen equivalents of phytoestrogens included in each CRF-1 and soy-free diet were roughly calculated as 0.91 and 0.06 ppm of β-estradiol, respectively, based on the relative binding affinities in a rat endometrial-derived experimental model [24]. Nutritional standards did not differ between soy-free diet and CRF-1 (supplier's analysis).

2.2. Experimental design

The animal experiments were identical to those in a previous study [25]. In brief, maternal animals were randomly divided into four groups including untreated controls. Eight dams per group were treated with 200 ppm of MMI or 3 ppm or 12 ppm of PTU in the drinking water from GD 10 to PND 20. Dose finding study on PTU and MMI was preliminarily performed based on the dose range to show changes in neuronal or oligodendroglial parameters in previous reports [2,26–28]. With the dose setting at the level of 9 ppm or 12 ppm for PTU and 200 ppm or 250 ppm for MMI in the drinking water, dams ($n = 2$/dose) were treated from GD 10 to PND 20, apart from the untreated control dams ($n = 2$). As a result, PTU at 12 ppm and MMI at 200 ppm exhibited clear hypothyroidism-linked effects to dams, i.e., increased relative thyroid weights and thyroid follicular cell hypertrophy, but did not affect pregnancy, implantation, delivery, or nursing until PND 20 (data not shown).

On PND 2, the litters were culled randomly, leaving four male and four female offspring. On PND 20, 20 male and 20 female offspring (at least one male and one female per dam) per group were subjected to prepubertal necropsy [25,29].

The remaining animals were maintained until postnatal week (PNW) 11. All offspring consumed the CRF-1 basal diet and tap water *ad libitum* from PND 20 onwards. At PNW 11, all pups were subjected to adult stage necropsy [25,29].

All animals used in the present study were weighed and sacrificed by exsanguination from the abdominal aorta under deep anesthesia with ether. These protocols were reviewed in terms of animal welfare and approved by the Animal Care and Use Committee of the National Institute of Health Sciences, Japan.

2.3. Thyroid-related hormone measurement

At the necropsies of animals sacrificed on PND 20 and PNW 11, blood samples of male offspring were collected from the abdominal aorta under anesthesia. Serum was prepared and stored at −30 °C to measure thyroid-stimulating hormone (TSH), triiodothyronine (T_3) and thyroxine (T_4) concentrations at SRL, Inc. (Tokyo, Japan). Number of animals examined was described in Table 1.

2.4. Immunohistochemistry and Cresyl Violet staining

To evaluate the immunohistochemical distribution of the molecules, brains in the subgroups of male offspring killed at PND 20 and PNW 11 were fixed in Bouin's solution at room temperature overnight. Six animals were used as untreated controls, six for 200 ppm MMI, eight for 3 ppm PTU, and nine for 12 ppm PTU on PND 20.

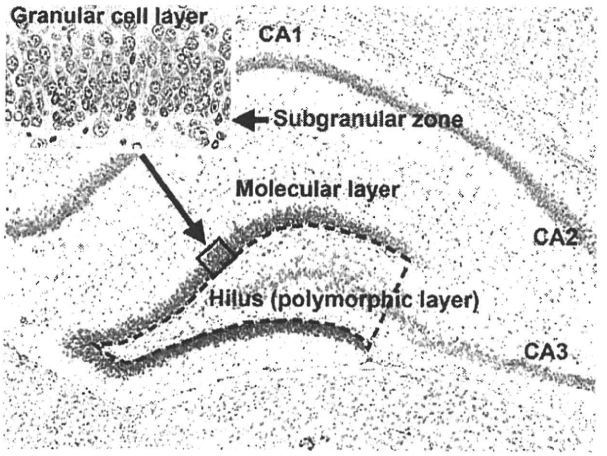

Fig. 1. Overview of the hippocampal formation of a male rat at postnatal day 20 stained with hematoxylin and eosin. Inset shows higher magnification of the granular cell layer and subgranular zone. Magnification, 40× (Inset: 200×). Number of immunoreactive cells for Reelin, Calb-D-28K, and GAD67 in the hilus of the dentate gyrus, as enclosed by the dotted line, was counted and normalized for the unit area. Small-sized neurons in this area showed positive immunoreactivity with these antigens, but large-sized CA3 neurons distributed in this area were not immunoreactive with these antigens. Number of NeuN-immunoreactive cells was similarly counted and normalized for the unit area, but CA3 neurons distributed in this area and also positive for NeuN were excluded from counting.

On PNW 11, 10 animals were used as untreated controls and 10 for 200 ppm MMI, nine for 3 ppm PTU, and six for 12 ppm PTU. Coronal slices at the positions of −3.0 and −3.5 mm from the bregma were prepared from brains of PND 20 and PNW 11, respectively.

Immunohistochemistry was performed on the brain sections (3 μm in thickness) of PND 20 and PNW 11 animals with antibodies against Reelin (clone G10, mouse $IgG_{1\kappa}$, 1:1000; Novus Biologicals, Inc., Littleton, CO, USA) and Calbindin-D-28K (Calb-D-28K; clone CB-955, mouse IgG_1, 1:500; Sigma Chemical Co.), which were incubated with the tissue sections overnight at 4 °C. On the brain sections at PNW 11, immunohistochemistry of neuron-specific nuclear protein (NeuN; clone A60, mouse IgG_1, 1:1000, Chemicon, Billerica, MA, USA), which specifically detects postmitotic neurons, was also performed. In addition, immunohistochemistry of glutamic acid decarboxylase 67 (GAD67; clone 1G10.2, mouse IgG, 1:50, Chemicon) and proliferating cell nuclear antigen (PCNA; clone PC10, mouse IgG_{2a}, 1:200, Dako, Glostrup, Denmark) was performed on PND 20 and PNW 11 ($n=5$ in each group) in untreated controls and rats treated with 12 ppm PTU. Antigen retrieval treatment was not performed for these antigens. Immunodetection was carried out using a VECTASTAIN® Elite ABC kit (Vector Laboratories Inc., Burlingame, CA, USA) with 3,3′-diaminobenzidine/H_2O_2 as the chromogen, as previously described [30]. The sections were then counterstained with hematoxylin and coverslipped for microscopic examination.

For double staining of NeuN and Reelin, 3,3′,5,5′-tetramethylbenzidine (Vector Laboratories) was used to visualize Reelin and DAB was used to visualize NeuN.

For evaluation of apoptosis in the subgranular zone of the dentate gyrus, apoptotic bodies were detected by Cresyl Violet staining as described by others [31].

2.5. Morphometry of immunolocalized cells and apoptotic cells

Reelin-, NeuN-, Calb-D-28K- or GAD67-positive cells distributed in the hilus of the dentate gyrus were bilaterally counted and normalized for the number per unit area of the hilar area (polymorphic layer) as enclosed by the dotted line in Fig. 1. In the subgranular zone of the dentate gyrus (Inset of Fig. 1), apoptotic bodies as detected by Cresyl Violet staining and proliferating cells as detected by nuclear immunoreactivity of PCNA were bilaterally counted and normalized the number with the length of the granular cell layer measured. For quantitative measurement of each immunoreactive cellular component, digital photomicrographs at 100-fold magnification were taken using a BX51 microscope (Olympus Optical Co., Ltd., Tokyo, Japan) attached to a DP70 Digital Camera System (Olympus Optical Co.), and quantitative measurements were performed using the WinROOF image analysis software package (version 5.7, Mitani Corp., Fukui, Japan).

2.6. Statistical analysis

Numerical data of the thyroid-related hormone levels and the number of immunoreactive cells were assessed using Student's *t*-test to compare the untreated controls with each of the anti-thyroid agent-exposed groups when the variance was homogenous among the groups using a test for equal variance. If a significant difference in variance was observed, Aspin–Welch's *t*-test was used instead.

3. Results

3.1. Effects on dams

During the gestation period, slight but statistically significant decrease of water consumption during GD 10–GD 15 and food intake during GD 15–GD 20 were observed with 200 ppm MMI compared with the untreated dams [25]. During the lactation period, both water consumption and food intake of dams decreased with 12 ppm PTU and MMI with statistical significance. However, treatment did not affect the body weight gain during the exposure period and the body weight of dams at weaning [25]. With regard to the maternal clinical signs, all dams in the groups of 12 ppm PTU and MMI exhibited somewhat higher sensitivity against handling stimuli as compared with untreated controls and 3 ppm PTU after delivery. However, no dams abandoned rearing offspring.

By monitoring water consumption, chemical intake of dams treated with 3 ppm PTU was calculated to be 0.57 mg/kg body weight/day during the whole exposure period (0.39 mg/kg body weight/day during GD 10–GD 20 and 0.67 mg/kg body weight/day during PND 1–PND 20) [25]. In case of dams treated with 12 ppm PTU, intake value was 1.97 mg/kg body weight/day during the whole exposure period (1.54 mg/kg body weight/day during GD 10–GD 20 and 2.20 mg/kg body weight/day during PND 1–PND 20). In case of dams treated with 200 ppm MMI, intake value was 27.2 mg/kg body weight/day during the whole exposure period (19.7 mg/kg body weight/day during GD 10–GD 20 and 31.2 mg/kg body weight/day during PND 1–PND 20).

3.2. Effects on offspring growth and survival

With regard to the reproductive parameters, no significant alterations in the number of implantation sites, number of live offspring, and sex ratio were observed by the exposure to anti-thyroid agents. At PND 1, a slight and non-significant decrease of the body weight was observed in all exposure groups of both sexes [25]. All animals survived during the lactation period. At PND 20, a decrease of body weight was observed after exposure to anti-thyroid agents in both sexes, which was statistically significant in the males of the 12 ppm PTU and MMI groups and in females of all exposure groups. After weaning, four out of ten males and six out of ten females receiving 12 ppm PTU were found dead or subjected to moribund sacrifice. During observation, many of these animals were hyperactive and aggressive in nature and sometimes raced around to bump into a cage wall. During necropsy, most of these animals showed evidence of acute hemorrhage of the brain surface.

At the necropsy of 11-week rats, only six males and four females remained in the 12 ppm PTU group, whereas 10 animals/sex remained in other groups. Offspring of dams receiving 12 ppm PTU and MMI showed a statistically significant decrease in body weight in both sexes [25].

3.3. Serum levels of thyroid-related hormones

At PND 20, decreases of serum levels of T_3 and T_4 were evident in animals that were administered anti-thyroid agents with statistical significance in all groups of animals exposed to anti-thyroid agents for both T_3 and T_4 (Table 1). Reductions of T_3 and T_4 with PTU occurred in a dose-dependent fashion. Significantly elevated TSH levels were observed with MMI and PTU at both doses. At PNW 11, a slight but statistically significant decrease of T_3 levels was observed with MMI and 12 ppm PTU groups.

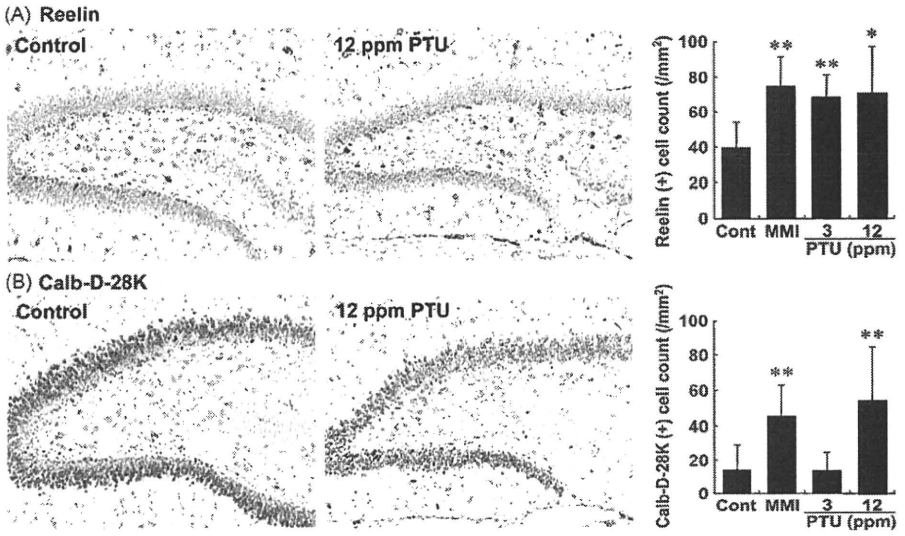

Fig. 2. Distribution of immunoreactive cells for Reelin and Calb-D-28K in the hippocampal formation in male rats at PND 20 after maternal exposure to anti-thyroid agents. (A) Reelin-immunoreactive cells in the hilus of the dentate gyrus. Reelin-positive cells with abundant cytoplasm show scattered distribution within the hilar region of the dentate gyrus. Note the higher number of Reelin-positive cells in a case exposed to 12 ppm PTU (Right) as compared with the control animal (Left). Magnification, 100×. The graph shows the number of Reelin-positive cells/unit area (mm^2) of the hilus of the bilateral hemispheres. $^*P<0.05$, $^{**}P<0.01$ *versus* untreated controls. (B) Calb-D-28K-immunoreactive cells in the hilus of the dentate gyrus. Calb-D-28K-positive cells are mainly distributed in the area medial to the subgranular zone. Note the higher number of Calb-D-28K-positive cells in a case exposed to 12 ppm PTU (Right) as compared with the control animal (Left). Magnification, 100×. The graph shows the number of Calb-D-28K-positive cells/unit area (mm^2) of the hilus of the bilateral hemispheres. $^{**}P<0.01$ *versus* untreated controls.

3.4. Immunolocalization of Reelin and Calb-D-28K in the hippocampal formation at PND 20

The distribution of Reelin-immunoreactive cells in the hippocampal formation that included the CA1–3 regions was similar to that described in the literature [14]. In the dentate gyrus, Reelin was expressed predominantly in the interneurons located in the hilus (polymorphic layer), whereas Reelin-containing neurons were sparse in the molecular layer (Fig. 2A). Morphometrically, the number of Reelin-positive cells in the dentate hilus was normalized in terms of unit area, and all of the animals exposed to MMI or PTU showed an increased number of Reelin-positive cells with a rather diffuse distribution within the hilus.

With regard to Calb-D-28K, the CA1 pyramidal neurons expressed this molecule with intense immunoreactivity in the inner pyramidal cells. Within the dentate gyrus, neurons in the granular cell layer showed strong immunoreactivity, while cells in the subgranular zone showed no expression (Fig. 2B). In addition to Reelin, Calb-D-28K-immunoreactive cells were frequently observed in the dentate hilus at the position medial to the subgranular zone. As compared with the untreated controls, animals exposed to MMI or 12 ppm PTU exhibited an increased number of Calb-D-28K-positive cells in the dentate hilus, while 3 ppm PTU did not show any change.

3.5. Immunolocalization of Reelin and Calb-D-28K in the hippocampal formation at PNW 11

On PNW 11, Reelin-immunoreactive cells showed similar distributions to those at PND 20 within the hippocampal formation, although the total number was reduced in the CA1–3 regions, by contrast to the comparable numbers in the dentate gyrus at PND 20. In the hilus of the dentate gyrus, the immunoreactive cells were increased in the MMI- and both doses of PTU-exposed animals (Fig. 3).

There were no cells immunoreactive for Calb-D-28K in the hippocampal formation in both untreated controls and MMI or PTU-exposed animals.

3.6. Characterization of the neuronal cell population in the dentate hilus

Within the hilus of the dentate gyrus, the number of NeuN-positive cells was apparently increased in the MMI- and both doses of PTU-exposed animals at PNW 11 as indicated by solid line in Fig. 4A.

The number of GAD67-positive cells in the animals treated with 12 ppm PTU tended to increase at PNW 11 compared with untreated controls, but was unchanged at PND 20 (Fig. 4B, C).

Evaluation of the co-localization of Reelin and NeuN in the dentate hilus at PNW 11 in untreated controls and 12 ppm PTU-exposed animals revealed that more than half of the Reelin-positive cells were weakly positive (±) or negative (−) for NeuN in the untreated controls, and 12 ppm PTU apparently increased this cell population (Fig. 4D).

3.7. Apoptotic and proliferating cell indices in the dentate subgranular zone

Apoptotic bodies were not found in the subgranular zone of the untreated controls at PND 20 (Fig. 5A). Also, no apoptotic bodies were detected after exposure to 3 ppm PTU at this time point. Although the number was very few, apoptotic bodies were increased after exposure to 12 ppm PTU. MMI-exposed animals also showed an increasing tendency in the number of apoptotic bodies. At PNW 11, no apoptotic bodies were detected in all cases including untreated controls, except for one apoptotic body detected in one case out of six untreated control animals.

With regard to the PCNA-immunoreactivity in the subgranular zone in untreated control animals, positive nuclei were sparsely observed at PND 20, and the number was decreased at PNW 11 (Fig. 5B). When the number of PCNA-immunoreactive nuclei was compared between the untreated controls and 12 ppm PTU, the latter decreased the number at PND 20. On the other hand, at PNW 11, no statistical difference was observed in the number of immunoreactive cells between the two groups.

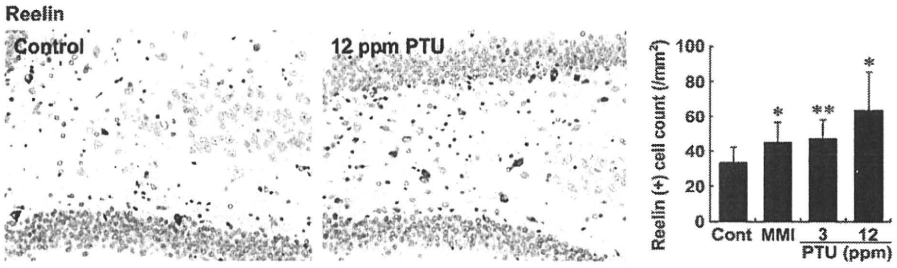

Fig. 3. Distribution of immunoreactive cells for Reelin in the hilus of the hippocampal dentate gyrus at PNW 11 of male rats exposed maternally to anti-thyroid agents. Similar to PND 20, the Reelin-positive cells with abundant cytoplasm show a scattered distribution within the hilar region of the dentate gyrus. Note the higher number of Reelin-positive cells in a case exposed to 12 ppm PTU (Right) as compared with the control animal (Left). Magnification, 100×. The graph shows the number of Reelin-positive cells/unit area (mm^2) of the hilus of the bilateral hemispheres. $^*P<0.05$, $^{**}P<0.01$ *versus* untreated controls.

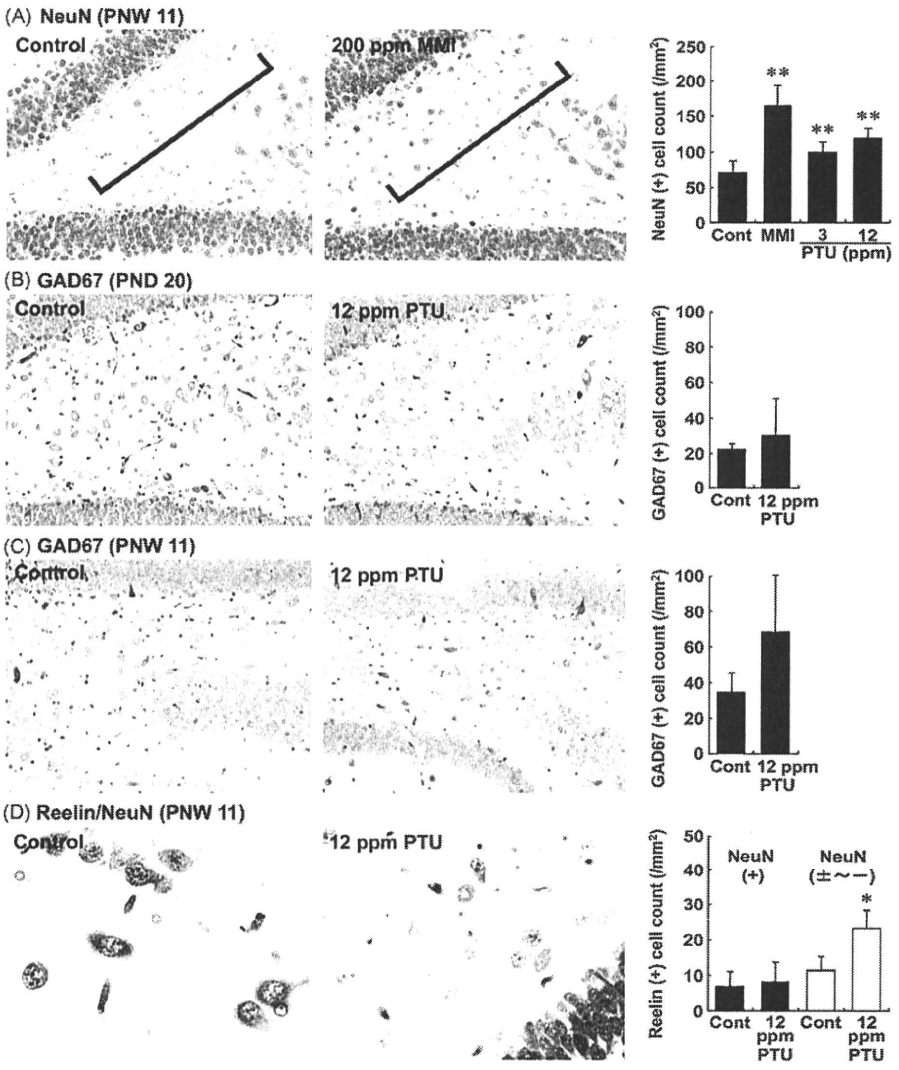

Fig. 4. Distribution of immunoreactive cells for NeuN and GAD67, and co-localization of Reelin and NeuN in the dentate hilus of male rats exposed maternally to anti-thyroid agents. (A) NeuN-immunoreactive cells at PNW 11. NeuN-positive cells are mainly distributed in the hilar area medial to the subgranular zone. Note the higher number of NeuN-positive cells in a case exposed to 200 ppm MMI (Right) as compared with the control animal (Left). Magnification, 200×. The graph shows the number of NeuN-positive cells/unit area (mm^2) of the hilus of the bilateral hemispheres. $^{**}P<0.01$ *versus* untreated controls. (B) GAD67-immunoreactive cells at PND 20. GAD67-positive cells with abundant cytoplasm show a scattered distribution within the hilar region. Magnification, 200×. Note there is no change in the number of GAD67-positive cells in a case exposed to 12 ppm PTU (Right) as compared with the control animal (Left). The graph shows the number of GAD67-positive cells/unit area (mm^2) of the hilus of bilateral hemispheres. (C) GAD67-immunoreactive cells at PNW 11. Similar to the PND 20 cases, the GAD67-positive cells with abundant cytoplasm show a scattered distribution within the hilar region. Magnification, 200×. Note the higher number of GAD67-positive cells in a case exposed to 12 ppm PTU (Right) as compared with the control animal (Left). The graph shows the number of GAD67-positive cells/unit area (mm^2) of the hilus of the bilateral hemispheres. (D) Double staining of Reelin and NeuN at PNW 11. Magnification, 600× (Left); 400× (Right). Note the increased number of Reelin-positive cells showing weak or no immunoreactivity for NeuN in a case exposed to 12 ppm PTU (Right) as compared with the control animal (Left). The graph shows the number of Reelin-positive cells with apparent (+) or weak to negative (±~−) NeuN-immunoreactivity/unit area (mm^2) of the hilus of the bilateral hemispheres. $^*P<0.01$ *versus* untreated controls.

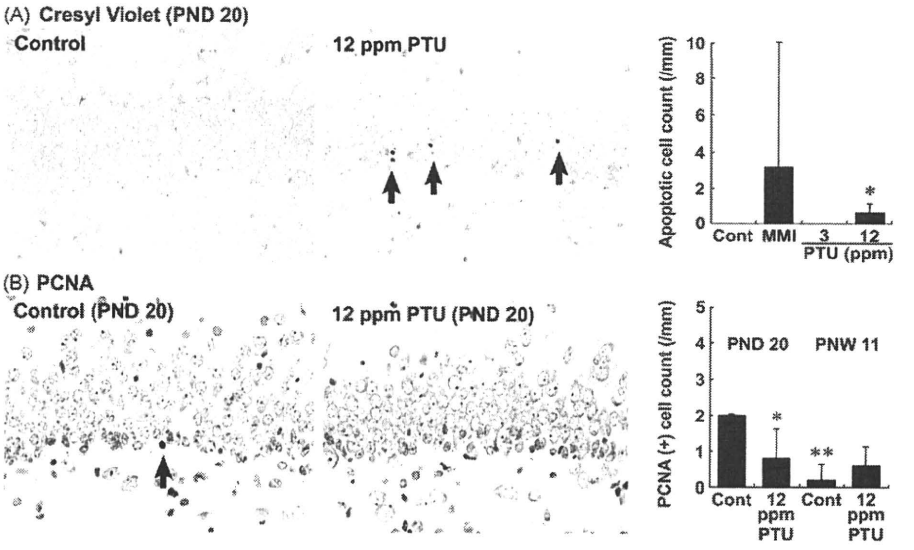

Fig. 5. Distribution of apoptotic cells and proliferating cells in the dentate subgranular zone of male rats exposed maternally to anti-thyroid agents. (A) Apoptotic cells detected as apoptotic bodies with Cresyl Violet staining at PND 20. Note sparse distribution of apoptotic bodies (arrows) in a case exposed to 12 ppm PTU (Right) as compared with the control animal without apoptotic bodies (Left). Magnification, 400×. The graph shows the number of apoptotic bodies/unit length (mm) of the subgranular zone of bilateral hemispheres at PND 20. $^{*}P<0.05$ *versus* untreated controls. (B) Proliferating cells as detected by PCNA-positive nuclei at PND 20. Note one PCNA-positive nucleus (arrow) in the micrographic view of the control animal (Left), while no positive nuclei were found in a case of 12 ppm PTU (Right). Magnification, 400×. The graph shows the number of PCNA-positive nuclei/unit length (mm) of the subgranular zone of bilateral hemispheres at both PND 20 and PNW 11. $^{*}P<0.05$, $^{**}P<0.01$ *versus* untreated controls at PND 20.

4. Discussion

In our recent study using animals of the identical experiment of the present study, we detected typical hypothyroidism-related changes, such as thyroid follicular cell hypertrophy accompanied with increased thyroid weight, and fluctuations in the thyroid-related hormone levels at the end of maternal exposure to MMI or PTU [25]. Morphometrical analysis at the adult stage also revealed hypothyroidism-related brain changes reflecting neuronal mismigration [10] and impaired oligodendroglial development [2], in both chemicals, with PTU showing dose-dependence. Offspring also displayed evidence of growth retardation lasting into the adult stage with MMI and PTU at 12 ppm. Dams in these groups exhibited reductions in food intake and water consumption during the lactation period suggestive of the relation to the growth suppression of offspring. On the other hand, offspring exposed to 3 ppm PTU also exhibited reduced body weights at weaning, with a statistically significant difference in females, without a concurrent reduction of food intake and water consumption of dams, suggesting that the reduced body weight was due to the development of hypothyroidism [32].

With regard to male offspring exposed to 3 ppm PTU, a clear increase in Reelin-expressing cells was evident at the end of developmental exposure with the magnitude similar to other treatment groups, while body weight reduction with 3 ppm PTU was weak and non-significant. Increase of Reelin-expressing cells continued until adult stage in this group, irrespective of the no reduction in the terminal body weight. These results may suggest that the increase in Reelin-expressing cells was the reflection of hypothyroidism-related brain effect rather than systemic growth retardation. We recently found that experimental undernutrition of offspring during GD 10–PND 21 utilizing a rat intrauterine growth restriction model did not change the number of Reelin-expressing cells until adult stage (Ohishi and Shibutani, unpublished data).

During early postnatal life, Reelin expression becomes established in a subpopulation of GABAergic interneurons in the dentate gyrus, with a high density in the hilus and along the base of the granule cell layer [16], where Reelin is maintained throughout adult life [14,15]. In the present study, we also found an increase in Calb-D-28K-immunoeactive cells, as with Reelin-positive cells, in the dentate hilus after exposure to anti-thyroid agents at PND 20. Calcium binding protein Calb-D-28K and parvalbumin are known to form distinct subpopulations of GABAergic interneurons in the rodent hippocampal formation [33]. During early postnatal development in human, subpopulations of Reelin-positive interneurons express Calb-D-28K in the dentate hilus [34]. These results suggest that the increased Reelin-expressing cells in the dentate hilus at the end of developmental hypothyroidism in the present study are GABAergic interneurons. However, the Calb-D-28K-expressing cells disappeared at the adult stage, regardless of the presence of Reelin-expressing cells in the present study. Because aged rats lack Calb-D-28K expression in the hippocampal interneurons [35], Calb-D-28K may play a role in functional maturation of these cells [36]. Interestingly, experimental induction of epileptic seizures in rats facilitates neurogenesis of cells expressing Calb-D-28K in the dentate hilus [37,38].

In the adult stage, we also found increased numbers of Reelin-positive cells and NeuN-positive cells in the dentate hilus after developmental exposure to anti-thyroid agents. In parallel with the increase in NeuN-positive cells, the increased GAD67-positive population was confirmed in the 12 ppm PTU-exposed animals. On the other hand, double staining of Reelin and NeuN revealed that developmental hypothyroidism resulted in an increase in Reelin-positive cells showing weakly positive or negative NeuN-immunoreactivity. Faint expression of mature neuronal markers, such as NeuN and microtubule-associated protein-2, was reported to reflect immature nature of neurons [39]. These results suggest that developmental hypothyroidism resulted in a sustained increase in GABAergic interneurons in the dentate hilus until the adult stage, a subpopulation of these cells produced Reelin with immature neuronal nature.

In line with its role in neuronal migration during development, Reelin was reported to be involved in the rostral migratory stream

in adult rats [40]. Hippocampal heterotopias seen after exposure to methylazoxymethanol during uterine life [41] are not observed at birth but become progressively more evident between P5 and P21. Similarly, developmental hypothyroidism induced subcortical band heterotopia at weaning (PND 20), and this becomes more evident at the adult stage [25]. Because Reelin acts as a stop signal [42], postnatal overexpression of Reelin in the dentate hilus in the present study could be responsible for heterotopias by maintaining the migrating granular cells in an incorrect position.

On the other hand, the transient prenatal disturbance of neurogenesis by treatment with methylazoxymethanol induces a long-term increase in the number of neurons expressing Reelin in the hippocampus [43]. In the dentate gyrus, the neuronal stem/progenitor cells are located within the subgranular zone, and neurogenesis occurs constitutively throughout postnatal life in adult mammals [44]. During postnatal hypothyroidism, neural progenitor proliferation and differentiation have been shown to be impaired [3]. In the present study, we found a slight increase or increasing tendency in apoptotic cells as well as a slight suppression of cell proliferation activity in the dentate subgranular zone at PND 20 at the end of exposure to anti-thyroid agents, while these changes were not continued until adult stage. Similar supportive data have recently been reported showing gene expression changes suggestive of facilitation of apoptosis and suppression of cell proliferation in the hippocampal formation during the postnatal hypothyroidism and down-regulation of anti-apoptotic genes at the adult stage [20]. Thus, although the reason and consequence of overexpression of Reelin during adulthood is unclear, Reelin production can be sustained in later life in response to impaired neurogenesis as with mismigration in the dentate granular cells during development, and interneurons may play a role in sustained Reelin production. It is suggested that GABAergic inputs to dentate progenitor cells in adult stage promote activity-dependent neuronal differentiation [45].

5. Conclusions

In this study, we have shown persistent increases in GABAergic interneurons with Reelin production in an immature population until the adult stage in the dentate hilus after developmental hypothyroidism. These findings probably reflect a compensatory regulation for impaired neurogenesis and mismigration. There are many xenobiotic chemicals having a potential to interfere with thyroid hormone signaling in the developing brain. Considering an increasing demand to develop efficient screening method of developmental neurotoxicants, monitoring of Reelin-expressing interneurons in the hippocampal dentate hilus may provide a valuable tool for detection of chemicals that can affect neurogenesis and migration.

Conflict of interest

All of the authors disclose that there are no conflicts of interest that could inappropriately influence the outcomes of the present study.

Acknowledgments

We thank Miss Tomomi Morikawa for her technical assistance in conducting the animal study. We also thank Mrs. Shigeko Suzuki and Miss Ayako Kaneko for their technical assistance in preparing the histological specimens. This work was supported in part by Health and Labour Sciences Research Grants (Research on Risk of Chemical Substances) from the Ministry of Health, Labour and Welfare of Japan.

References

[1] Porterfield SP. Thyroidal dysfunction and environmental chemicals—potential impact on brain development. Environ Health Perspect 2000;108:433–8.
[2] Schoonover CM, Seibel MM, Jolson DM, Stack MJ, Rahman RJ, Jones SA, et al. Thyroid hormone regulates oligodendrocyte accumulation in developing rat brain white matter tracts. Endocrinology 2004;145:5013–20.
[3] Montero-Pedrazuela A, Venero C, Lavado-Autric R, Fernández-Lamo I, García-Verdugo JM, Bernal J, et al. Modulation of adult hippocampal neurogenesis by thyroid hormones: implications in depressive-like behavior. Mol Psychiatry 2006;11:361–71.
[4] de Escobar GM, Obregón MJ, del Rey FE. Iodine deficiency and brain development in the first half of pregnancy. Public Health Nutr 2007;10:1554–70.
[5] Asplund L, Svensson B, Eriksson U, Jansson B, Jensen S, Wideqvist U, et al. PCBs, DDT, DDE in human plasma related to fish consumption. Arch Environ Health 1994;49:477–86.
[6] Kodavanti PR, Ward TR, Derr-Yellin EC, Mundy WR, Casey AC, Bush B, et al. Congener-specific distribution of PCBs in brain regions, blood, liver, and fat of adult rats following repeated exposure to Aroclor 1254. Toxicol Appl Pharmacol 1998;153:199–210.
[7] Langer P. Review: persistent organochlorinated pollutants (POPs) and human thyroid—2005. Endocr Regul 2005;39:53–68.
[8] Comer CP, Norton S. Effects of perinatal methimazole exposure on a developmental test battery for neurobehavioral toxicity in rats. Toxicol Appl Pharmacol 1982;63:133–41.
[9] Akaike M, Kato N, Ohno H, Kobayashi T. Hyperactivity and spatial maze learning impairment of adult rats with temporary neonatal hypothyroidism. Neurotoxicol Teratol 1991;13:317–22.
[10] Lavado-Autric R, Ausó E, García-Velasco JV, Arufe Mdel C, del Rey FE, Berbel P, et al. Early maternal hypothyroxinemia alters histogenesis and cerebral cortex cytoarchitecture of the progeny. J Clin Invest 2003;111:954–7.
[11] Goodman JH, Gilbert ME. Modest thyroid hormone insufficiency during development induces a cellular malformation in the corpus callosum: a model of cortical dysplasia. Endocrinology 2007;148:2593–7.
[12] D'Arcangelo G, Miao GG, Chen SC, Soares HD, Morgan JI, Curran T. A protein related to extracellular matrix proteins deleted in the mouse mutant reeler. Nature 1995;374:719–23.
[13] D'Arcangelo G, Nakajima K, Miyata T, Ogawa M, Mikoshiba K, Curran T. Reelin is a secreted glycoprotein recognized by the CR-50 monoclonal antibody. J Neurosci 1997;17:23–31.
[14] Pesold C, Impagnatiello F, Pisu MG, Uzunov DP, Costa E, Guidotti A, et al. Reelin is preferentially expressed in neurons synthesizing γ-aminobutyric acid in cortex and hippocampus of adult rats. Proc Natl Acad Sci USA 1998;95:3221–6.
[15] Scotti AL, Herrmann G. Reelin immunoreactivity in dissociated cultures of the postnatal hippocampus. Brain Res 2002;924:209–18.
[16] Houser CR. Interneurons of the dentate gyrus: an overview of cell types, terminal fields and neurochemical identity. Prog Brain Res 2007;163:217–32.
[17] Alvarez-Dolado M, Ruiz M, Del Río JA, Alcántara S, Burgaya F, Sheldon M, et al. Thyroid hormone regulates reelin and dab1 expression during brain development. J Neurosci 1999;19:6979–93.
[18] Lussier AL, Caruncho HJ, Kalynchuk LE. Repeated exposure to corticosterone, but not restraint, decreases the number of reelin-positive cells in the adult rat hippocampus. Neurosci Lett 2009;460:170–4.
[19] Gong C, Wang TW, Huang HS, Parent JM. Reelin regulates neuronal progenitor migration in intact and epileptic hippocampus. J Neurosci 2007;27:1803–11.
[20] Zhang L, Blomgren K, Kuhn HG, Cooper-Kuhn CM. Effects of postnatal thyroid hormone deficiency on neurogenesis in the juvenile and adult rat. Neurobiol Dis 2009;34:366–74.
[21] Glass CK, Holloway JM, Devary OV, Rosenfeld MG. The thyroid hormone receptor binds with opposite transcriptional effects to a common sequence motif in thyroid hormone and estrogen response elements. Cell 1988;54:313–23.
[22] Zhu YS, Yen PM, Chin WW, Pfaff DW. Estrogen and thyroid hormone interaction on regulation of gene expression. Proc Natl Acad Sci USA 1996;93:12587–92.
[23] Masutomi N, Shibutani M, Takagi H, Uneyama C, Takahashi N, Hirose M. Impact of dietary exposure to methoxychlor, genistein, or diisononyl phthalate during the perinatal period on the development of the rat endocrine/reproductive systems in later life. Toxicology 2003;192:149–70.
[24] Hopert AC, Beyer A, Frank K, Strunck E, Wunsche W, Vollmer G. Characterization of estrogenicity of phytoestrogens in an endometrial-derived experimental model. Environ Health Perspect 1998;106:581–6.
[25] Shibutani M, Woo G-H, Fujimoto H, Saegusa Y, Takahashi M, Inoue K, et al. Assessment of developmental effects of hypothyroidism in rats from in utero and lactation exposure to anti-thyroid agents. Reprod Toxicol 2009;28:297–307.
[26] Barradas PC, Vieira RS, De Freitas MS. Selective effect of hypothyroidism on expression of myelin markers during development. J Neurosci Res 2001;66:254–61.
[27] Sawin S, Brodish P, Carter CS, Stanton ME, Lau C. Development of cholinergic neurons in rat brain regions: dose-dependent effects of propylthiouracil-induced hypothyroidism. Neurotoxicol Teratol 1998;20:627–35.
[28] Sui L, Anderson WL, Gilbert ME. Impairment in short-term but enhanced long-term synaptic potentiation and ERK activation in adult hippocampal area CA1 following developmental thyroid hormone insufficiency. Toxicol Sci 2005;85:647–56.

[29] Nakamura R, Teshima R, Hachisuka A, Sato Y, Takagi K, Nakamura R, et al. Effects of developmental hypothyroidism induced by maternal administration of methimazole or propylthiouracil on the immune system of rats. Int Immunopharmacol 2007;7:1630–8.
[30] Shibutani M, Lee K-Y, Igarashi K, Woo G-H, Inoue K, Nishimura T, et al. Hypothalamus region-specific global gene expression profiling in early stages of central endocrine disruption in rat neonates injected with estradiol benzoate or flutamide. Dev Neurobiol 2007;67:253–69.
[31] Nuñez JL, McCarthy MM. Cell death in the rat hippocampus in a model of prenatal brain injury: time course and expression of death-related proteins. Neuroscience 2004;129:393–402.
[32] Hapon MB, Simoncini M, Via G, Jahn GA. Effect of hypothyroidism on hormone profiles in virgin, pregnant and lactating rats, and on lactation. Reproduction 2003;126:371–82.
[33] Seress L, Gulyás AI, Ferrer I, Tunon T, Soriano E, Freund TF. Distribution, morphological features, and synaptic connections of parvalbumin- and calbindin D28k-immunoreactive neurons in the human hippocampal formation. J Comp Neurol 1993;337:208–30.
[34] Abraham H, Meyer G. Reelin-expressing neurons in the postnatal and adult human hippocampal formation. Hippocampus 2003;13:715–27.
[35] Potier B, Krzywkowski P, Lamour Y, Dutar P. Loss of calbindin-immunoreactivity in CA1 hippocampal stratum radiatum and stratum lacunosum-moleculare interneurons in the aged rat. Brain Res 1994;661:181–8.
[36] Grateron L, Cebada-Sanchez S, Marcos P, Mohedano-Moriano A, Insausti AM, Muñoz M, et al. Postnatal development of calcium-binding proteins immunoreactivity (parvalbumin, calbindin, calretinin) in the human entorhinal cortex. J Chem Neuroanat 2003;26:311–6.
[37] Scharfman HE, Goodman JH, Sollas AL. Granule-like neurons at the hilar/CA3 border after status epilepticus and their synchrony with area CA3 pyramidal cells: unctional implications of seizure-induced neurogenesis. J Neurosci 2000;20:6144–58.
[38] Scharfman HE, Sollas AL, Goodman JH. Spontaneous recurrent seizures after pilocarpine-induced status epilepticus activate calbindin-immunoreactive hilar cells of the rat dentate gyrus. Neuroscience 2002;111:71–81.
[39] Seki T. Expression patterns of immature neuronal markers PSA-NCAM, CRMP-4 and NeuroD in the hippocampus of young adult and aged rodents. J Neurosci Res 2002;70:327–34.
[40] Hack I, Bancila M, Loulier K, Carroll P, Cremer H. Reelin is a detachment signal in tangential chain-migration during postnatal neurogenesis. Nat Neurosci 2002;5:939–45.
[41] Baraban SC, Wenzel HJ, Hochman DW, Schwartzkroin PA. Characterization of heterotopic cell clusters in the hippocampus of rats exposed to methylazoxymethanol in utero. Epilepsy Res 2000;39:87–102.
[42] Frotscher M, Haas CA, Förster E. Reelin controls granule cell migration in the dentate gyrus by acting on the radial glial scaffold. Cereb Cortex 2003;13:634–40.
[43] Hoareau C, Hazane F, Le Pen G, Krebs MO. Postnatal effect of embryonic neurogenesis disturbance on reelin level in organotypic cultures of rat hippocampus. Brain Res 2006;1097:43–51.
[44] von Bohlen U, Halbach O. Immunohistological markers for staging neurogenesis in adult hippocampus. Cell Tissue Res 2007;329:409–20.
[45] Tozuka Y, Fukuda S, Namba T, Seki T, Hisatsune T. GABAergic excitation promotes neuronal differentiation in adult hippocampal progenitor cells. Neuron 2005;47:803–15.

Reproductive Toxicology 30 (2010) 591–599

Contents lists available at ScienceDirect

Reproductive Toxicology

journal homepage: www.elsevier.com/locate/reprotox

No effect of sustained systemic growth retardation on the distribution of Reelin-expressing interneurons in the neuron-producing hippocampal dentate gyrus in rats

Takumi Ohishi[a,b], Liyun Wang[a], Bunichiro Ogawa[a], Kenichi Fujisawa[b], Eriko Taniai[a,c], Hitomi Hayashi[a,c], Kunitoshi Mitsumori[a], Makoto Shibutani[a,*]

[a] Laboratory of Veterinary Pathology, Tokyo University of Agriculture and Technology, 3-5-8 Saiwai-cho, Fuchu-shi, Tokyo 183-8509, Japan
[b] Gotemba Laboratory, Bozo Research Center Inc., 1284 Kamado, Gotemba-shi, Shizuoka 412-0039, Japan
[c] Pathogenetic Veterinary Science, United Graduate School of Veterinary Sciences, Gifu University, 1-1 Yanagido, Gifu-shi, Gifu 501-1193, Japan

ARTICLE INFO

Article history:
Received 8 May 2010
Received in revised form 3 July 2010
Accepted 21 August 2010
Available online 27 October 2010

Keywords:
Developmental growth retardation
Maternal protein restriction
Hippocampal dentate gyrus
Reelin
γ-Aminobutyric acid (GABA)ergic interneuron
Neuronal migration
Neurogenesis

ABSTRACT

Reelin signaling plays a role in neuronal migration and positioning during brain development. To clarify the effect of systemic growth retardation on the distribution of Reelin-expressing interneurons in the hilus of the hippocampal dentate gyrus, pregnant rats were fed a synthetic diet with either a normal (20% casein) or low (10% casein) protein concentration from gestational day 10 to postnatal day (PND) 21 at weaning. Male offspring were immunohistochemically examined at PND 21 and on PND 77. Protein-restricted offspring displayed systemic growth retardation through PND 77 and had decreased absolute brain weights and an increased number of external granular cells in the cerebellar cortex, suggestive of retarded brain growth at weaning. However, maternal protein restriction did not change the cellular distribution of immunoreactivity for Reelin, Calbindin-D-28K, or glutamic acid decarboxylase 67 or of NeuN-positive postmitotic neurons in the dentate hilus either at PND 21 or PND 77, which suggests that the population of γ-aminobutyric acid-ergic interneurons involving synthesis of Reelin was not affected. Furthermore, as well as the distribution of hilar neurons expressing neurogenesis-related FoxG1, cell proliferation and apoptosis in the subgranular zone were unaffected through PND 77. These results suggest that systemic growth retardation caused by maternal protein restriction does not affect neuronal migration and postnatal neurogenesis of the dentate gyrus resulting in unaltered distribution of Reelin-synthesizing interneurons.

1. Introduction

In the hippocampal formation, neuronal subpopulations are known to produce Reelin from the embryonic period throughout adult life [1–5]. Reelin is a secreted extracellular matrix glycoprotein that plays a critical role in neuronal migration and positioning during brain development [2]. Its secretion is regulated by thyroid hormone [6]. Also, it has been suggested that Reelin release by γ-aminobutyric acid (GABA)ergic interneurons may regulate the migration and maturation of newborn granular cells in the dentate granular cell layer in adults [7]. Altered Reelin signaling has been reported in the dentate gyrus in some neurological disease conditions, such as depression and epilepsy [7,8]. Within the hippocampal formation, the dentate gyrus is a unique structure that can continue neurogenesis during postnatal life and that is a well-known target of developmental hypothyroidism [9].

Experimentally, developmental hypothyroidism leads to systemic growth retardation, neurological defects and impaired performance in a variety of behavioral learning tests [10,11]. The offspring of rats exposed to anti-thyroid agents such as 6-propyl-2-thiouracil (PTU) show impaired brain development, with aberrant neuronal migration and white matter hypoplasia involving limited axonal myelination and reduced oligodendrocytic distribution [12–14]. To detect a key molecular event reflecting the permanent disruption of neuronal development due to exposure to xenobiotic chemicals that can interfere with thyroid hormone signaling, we recently examined the change in the temporal distribution of Reelin-expressing cells in the dentate gyrus in the offspring of

Abbreviations: CA1, cornu ammonis 1; CA2, cornu ammonis 2; CA3, cornu ammonis 3; Calb-D-28K, Calbindin-D-28K; FoxG1, forkhead box G1; GABA, γ-aminobutyric acid; GAD67, glutamic acid decarboxylase 67; GD, gestational day; MMI, methimazole; NeuN, neuron-specific nuclear protein; PBS, phosphate buffered saline; PCNA, proliferating cell nuclear antigen; PND, postnatal day; PTU, 6-propyl-2-thiouracil; TUNEL, terminal deoxynucleotidyl transferase dUTP nick end labeling; T_3, triiodothyronine.

* Corresponding author. Tel.: +81 42 367 5874; fax: +81 42 367 5771.
E-mail address: mshibuta@cc.tuat.ac.jp (M. Shibutani).

0890-6238/$ – see front matter © 2010 Elsevier Inc. All rights reserved.
doi:10.1016/j.reprotox.2010.08.009

Table 1
Composition of normal and low protein diets.

	Normal protein diet (%)	Low protein diet (%)
Casein	20.00	10.00
L-Cystine	0.30	0.30
Corn starch	39.75	47.25
α-Corn starch	13.20	15.70
Sucrose	10.00	10.00
Soy oil	7.00	7.00
Cellulose	5.00	5.00
Mineral	3.50	3.50
Vitamin	1.00	1.00
Choline	0.25	0.25
tert-Butylhydroquinone	0.0014	0.0014

rats exposed to anti-thyroid agents during gestation and lactation [15]. As a result, an increase in GABAergic Reelin-synthesizing interneurons with immature phenotype that was sustained into the later stage at PND 77 was observed in the dentate hilus, which is suggestive of a compensatory mechanism for the impaired neurogenesis and mismigration caused by exposure to thyroid hormone-disrupting chemicals during neuronal development.

Systemic growth retardation of the offspring caused by maternal and/or offspring toxicity may cause a delay in brain development. In the above-mentioned study, we also observed a suppression of systemic growth in the offspring after exposure to anti-thyroid agents that caused apparent hypothyroidism in both dams and offspring [15,16]. It is possible that the sustained increase in Reelin-expressing cells is caused by the delayed brain growth accompanied by systemic growth retardation rather than the hypothyroidism-related impairment of thyroid hormone signaling in the brain. We also observed a sustained increase in Reelin-expressing cells even with mild hypothyroidism at a level that did not cause sustained body growth retardation through the later stage at PND 77. However, a slight, non-significant suppression of body growth was also detected in these animals at the end of developmental hypothyroidism on weaning. Because the high doses of chemicals in developmental toxicity studies sometimes cause systemic growth retardation of the offspring, any chemical-specific neurodevelopmental effects should be distinguished from those caused by systemic growth retardation resulting in delayed brain growth secondary to the systemic toxicity in dams and/or offspring.

In the present study, to clarify the effects of delayed brain growth on the distribution of Reelin-expressing interneurons in the dentate hilus, pregnant rats were fed a synthetic low-protein diet from the mid-gestation to the end of the lactation period to cause growth restriction in the offspring utilizing an intrauterine growth restriction model [17,18]. The distributional changes of GABAergic interneuron markers in the dentate hilus were investigated, as well as the effects on the neurogenesis of the subgranular zone in terms of cell proliferation and apoptosis.

2. Materials and methods

2.1. Animals, diets and experimental design

Pregnant Crl:CD®(SD) rats were purchased from Charles River Japan Inc. (Yokohama, Japan) at gestational day (GD) 1 (appearance of vaginal plugs was designated as GD 0). Animals were housed individually in mesh cages in an air-conditioned animal room (temperature: 23 ± 2 °C; relative humidity: 45 ± 10%) with a 12-h light/dark cycle and were allowed *ad libitum* access to food and tap water. Animals were housed individually with their litter in plastic cages with wood chip bedding from GD 17 to postnatal day (PND) 21 (PND 0: the day of birth).

Pregnant rats were fed a CRF-1 basal diet (Oriental Yeast Co. Ltd.) from GD 1 to GD 10. Eight dams per group were then randomly divided into two groups and fed a synthetic diet with either a normal (20% casein) or a low (10% casein) protein concentration from GD 10 to PND 21. Compositions of the synthetic diets are shown in Table 1.

On PND 4, the litters were culled randomly, leaving four male and four female offspring per dam. On PND 21, 10 male and 10 female offspring per group from 8 dams (one or two males and one or two females per dam) were subjected to prepubertal necropsy.

The remaining animals were kept until PND 77. All offspring consumed the CRF-1 basal diet and tap water *ad libitum* from PND 21 onwards. On PND 77, 10 male and 10 female offspring per group from 8 dams (one or two males and one or two females per dam) were subjected to necropsy [16,19].

All animals used in the present study were weighed and killed by exsanguination from the abdominal aorta under deep anesthesia with ether. All procedures of this study were conducted in compliance with the "Guidelines for Proper Conduct of Animal Experiments" (Science Council of Japan, June 1, 2006) and according to the protocol approved by the Animal Care and Use Committee at BOZO Research Center Inc. All efforts were made to minimize animal suffering.

2.2. Histopathology, immunohistochemistry and apoptotic cell detection

The brains of the male offspring killed at PND 21 and PND 77 were fixed in Bouin's solution at room temperature overnight. Ten identical male animals from 8 dams (one or two males per dam) per group were subjected to analyses on histopathology, immunohistochemistry and apoptotic cell detection at each time point. Coronal slices at the positions of −3.0 and −3.5 mm from the bregma were prepared from the PND 21 and PND 77 brains, respectively. Brains were routinely processed for paraffin embedding, sectioned at 3 μm, and stained with hematoxylin and eosin for light microscopy.

For immunohistochemistry studies, the brain sections (3 μm in thickness) were incubated at 4 °C overnight with antibodies against Reelin (clone G10, mouse IgG_1, 1:1,000; Novus Biologicals, Inc., Littleton, CO, United States), neuron-specific nuclear protein (NeuN; clone A60, mouse IgG_1, 1:100, Millipore Corporation, Temecula, CA, United States), which specifically detects postmitotic neurons [20], calbindin-D-28K (Calb-D-28K; clone CB-955, mouse IgG_1, 1:500; Sigma Chemical Co., St. Louis, MO, United States), a Ca-binding protein that is expressed in the GABAergic interneurons [21], glutamic acid decarboxylase 67 (GAD67; clone 1G10.2, mouse IgG_{2a}, 1:50, Millipore Corporation), a GABA synthesizing enzyme that is expressed in GABAergic neurons [22], forkhead box G1 (FoxG1; rabbit IgG, 1:800; LifeSpan Bioscience, Inc., Seattle, WA, United States), a transcription factor that regulates neurogenesis in the embryonic telencephalon and the postnatal hippocampus [23,24], and proliferating cell nuclear antigen (PCNA; clone PC10, mouse IgG_{2a}, 1:200, Dako, Glostrup, Denmark). Antigen retrieval treatment was not performed for these antigens. To quench endogenous peroxidase, the slides were incubated in 0.3% hydrogen peroxide in absolute methanol for 30 min. Immunodetection was carried out using a VECTASTAIN® Elite ABC kit (Vector Laboratories Inc., Burlingame, CA, United States) with 3,3′-diaminobenzidine/H_2O_2 as the chromogen, as previously described [25]. The sections were then counterstained with hematoxylin and coverslipped for microscopic examination.

For evaluation of apoptosis in the subgranular zone of the dentate gyrus, a terminal deoxynucleotidyl transferase dUTP nick end labeling (TUNEL) assay was applied to brain sections. Deparaffinized sections were treated with 20 μg/mL of proteinase K in phosphate buffered saline (PBS; pH 7.4) for 15 min at room temperature, and then incubated in 3.0% hydrogen peroxide in PBS for 5 min. Detection of apoptotic cells was carried out using the Apop Tag® *in situ* apoptosis detection kit (Millipore Corporation) according to the instructions provided by the manufacturer with 3,3′-diaminobenzidine/H_2O_2 as the chromogen.

2.3. Morphometry of immunolocalized cells and apoptotic cells

Reelin-, NeuN-, Calb-D-28K-, GAD67- or FoxG1-positive cells distributed in the hilus of the dentate gyrus were bilaterally counted and normalized for the number per area unit of the hilar area (polymorphic layer) as previously described [15]. In the subgranular zone of the dentate gyrus, apoptotic cells as detected by TUNEL method and proliferating cells as detected by nuclear immunoreactivity of PCNA were bilaterally counted and normalized for the length of the granular cell layer measured as previously described [15]. For quantitative measurement of each immunoreactive cellular component, digital photomicrographs at 100-fold magnification were taken using a BX51 microscope (Olympus Optical Co., Ltd., Tokyo, Japan) attached to a DP70 Digital Camera System (Olympus Optical Co.). Quantitative measurements were performed using the WinROOF image analysis software package (version 5.7, Mitani Corp., Fukui, Japan).

2.4. Statistical analysis

Maternal data regarding the body weight and food consumption during the animal study were analyzed using the individual animal as the experimental unit. Data for offspring regarding the body weight, food consumption, organ weight at necropsy, immunohistochemical data, and TUNEL-assay data, were analyzed using the litter as the experimental unit. Differences between the normal and low protein diet groups were evaluated using the following methods. An *F*-test for equal variance was used to determine if the variance was homogenous between the groups. If the variance was homogenous, numerical data were assessed using Student's *t*-test to compare between the normal and low protein diet groups. If a significant difference in variance was observed, the Aspin–Welch's *t*-test was used instead.

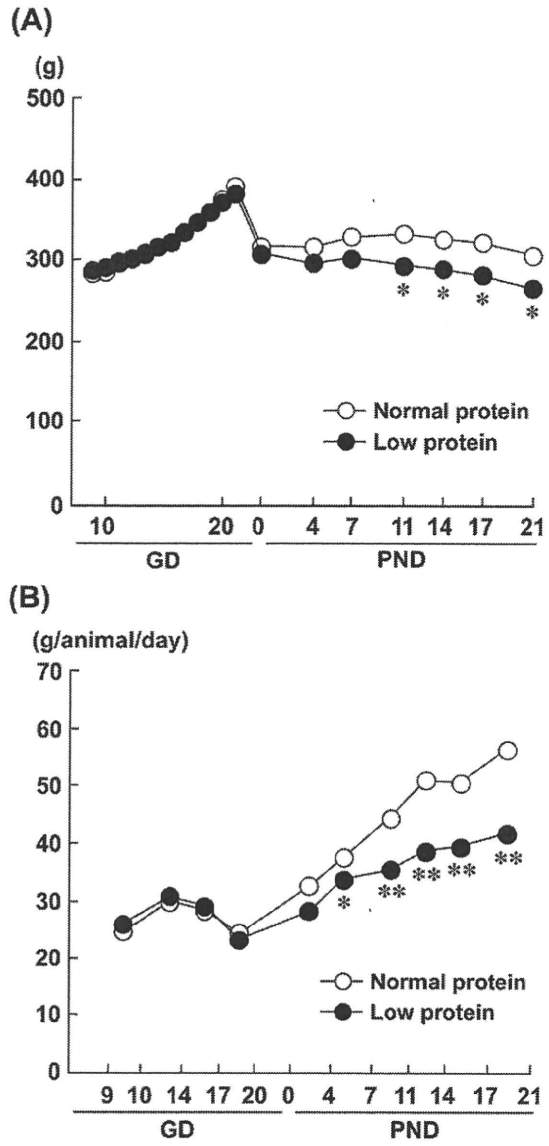

Fig. 1. Body weights and food consumption of dams fed either a normal or low protein diet from GD 10 to PND 21. (A) Body weight. (B) Food consumption. *,** Significantly different from the normal protein group by Student's or Aspin–Welch's *t*-test (*$P < 0.05$; **$P < 0.01$).

Data for offspring regarding the incidences and severity of histopathological lesions were analyzed using the individual animal as the experimental unit. The incidences of histopathological lesions were statistically compared using the Fisher's exact probability test. Severity of histopathological changes was compared using the Mann–Whitney's *U*-test.

3. Results

3.1. Effects on dams

During the gestational period, there were no statistically significant differences in body weight and food consumption between the normal and low protein diet groups (Fig. 1). During the lactation period, body weights of dams and food consumption per animal were significantly lower in the low protein diet group than in the normal protein diet group from PND 11 and PND 4 onwards, respectively (Fig. 1). Food consumption per body weight was also decreased from PND 11 to PND 21 (data not shown).

3.2. Effects on offspring growth

Throughout the lactation period, body weights of the offspring of both sexes were significantly lower in the low protein diet group than in the normal protein diet group (Table 2).

After weaning, body weights were significantly lower in the low protein group than in the normal protein diet group in both sexes through PND 77 (Table 2). Food consumption per animal was suppressed in the low protein group from PND 35 to PND 77 in males and from PND 56 to PND 77 in females (Table 3). Conversely, food consumption per body weight was increased in the low protein diet group from PND 35 to PND 63 and on PND 77 in males and from PND 35 to PND 49 in females.

3.3. Effects on organ weights of the offspring

At necropsy on PND 21, statistically significant decreases in the absolute brain and liver weights were observed in both sexes in the low protein diet group (Table 4). However, relative brain weights in both sexes and relative liver weights in males were significantly increased in the low protein diet group.

At necropsy on PND 77, statistically significant decreases in the absolute kidney weights in both sexes and liver and testes weights in males were observed in the low protein diet group. However, relative brain weights were significantly increased in males in the low protein diet group.

3.4. Histopathological changes

On histopathological analysis of the pups on PND 21, the grade of external granular cells remaining in the cerebellar cortex in the low protein group was significantly higher than in the normal protein group (Table 5).

On PND 77, there were no histopathological alterations in the brains of both low and normal protein diet groups.

3.5. Morphometry of immunolocalized cells in the dentate gyrus

On PND 21, Reelin expression was observed in the cytoplasm of neurons located within the dentate hilus (Fig. 2). Immunoreactivity for NeuN was observed exclusively in the nucleus of granular cells but not in cells located in the subgranular zone. NeuN-positive neurons were also observed within the dentate hilus, showing cytoplasmic immunoreactivity in addition to nuclear immunolocalization, as reported by others [26]. Calb-D-28K was expressed in both the cytoplasm and the nucleus in the granular cells and neurons within the dentate hilus. GAD67-expression was observed in the cytoplasm of the neurons located in the hilus and those sparsely distributed in the granular cell layer. FoxG1 expression was observed in the cytoplasm in neurons within the hilus and in granular cells, except for the cells located at the subgranular zone. There were no differences in the number of Reelin-, NeuN-, Calb-D-28K-, GAD67- or FoxG1-positive cells distributed in the hilus of the dentate gyrus between the normal and low protein diet groups (Fig. 2).

On PND 77, the cellular distribution of each molecule was similar to that observed on PND 21, while cells located in the subgranular zone were reduced, judging from the very sparse distribution of negative cells for NeuN and FoxG1 (Fig. 3). Within the dentate hilus, the number of positive cells for each molecule was lower on PND 77 than on PND 21. As on PND 21, there were no differences in the number of positive cells for any of the molecules in the dentate hilus between the normal and low protein diet groups (Fig. 3).

Table 2
Body weight of offspring after maternal protein restriction during the second half of gestation and lactation.

	Males		Females	
	Normal protein20%[c]	Low protein10%[c]	Normal protein20%[c]	Low protein 10%[c]
No. of offspring examined[a]	16	16	16	16
Body weight (g)				
PND 0	6.6 ± 0.6[b]	6.3 ± 0.4**	6.1 ± 0.4	5.9 ± 0.5*
PND 4	10.9 ± 1.4	9.0 ± 1.1**	10.4 ± 1.5	8.5 ± 1.0**
PND 7	17.5 ± 2.3	13.7 ± 1.9**	16.4 ± 2.6	12.4 ± 1.8**
PND 11	28.9 ± 3.6	21.4 ± 1.6**	27.0 ± 3.7	19.2 ± 2.3**
PND 14	38.4 ± 4.4	26.6 ± 1.5**	36.2 ± 3.9	24.5 ± 2.3**
PND 17	46.5 ± 5.5	31.6 ± 1.9**	43.9 ± 4.5	29.2 ± 2.5**
PND 21	61.4 ± 7.0	40.4 ± 2.4**	58.0 ± 6.1	38.0 ± 3.6**
PND 28	102.8 ± 10.9	75.4 ± 4.7**	90.1 ± 9.6	70.8 ± 4.1**
PND 35	174.5 ± 16.3	136.5 ± 8.1**	142.3 ± 12.3	121.4 ± 6.6**
PND 42	253.0 ± 19.6	203.1 ± 9.6**	181.3 ± 12.4	160.6 ± 8.4**
PND 49	322.8 ± 21.7	263.2 ± 13.6**	206.2 ± 13.6	187.5 ± 12.1**
PND 56	382.8 ± 22.1	318.6 ± 15.0**	228.7 ± 14.4	207.2 ± 15.1**
PND 63	429.4 ± 25.9	358.9 ± 20.5**	255.4 ± 19.1	231.1 ± 18.8**
PND 70	474.5 ± 28.0	398.3 ± 23.1**	276.8 ± 23.3	247.4 ± 20.4*
PND 77	508.3 ± 30.6	427.0 ± 26.9**	285.3 ± 22.5	254.9 ± 22.6*

*, **Significantly different from the normal protein group by Student's or Aspin–Welch's *t*-test ($P < 0.05$; $P < 0.01$).
Abbreviation: PND, postnatal day.
[a] Identical two male and two female offspring per dam ($n = 8$/group) were used for body weight measurement throughout the experiment. Statistical analysis was performed using the litter as the experimental unit.
[b] Mean ± SD.
[c] Casein level.

3.6. Apoptotic and proliferating cell indices in the dentate subgranular zone

On PND 21, there were very few TUNEL-positive apoptotic cells in the subgranular zone of the dentate gyrus, and there was no difference in the number per unit length between the normal and low protein diet groups (Fig. 4). There were no differences in the number of PCNA-positive cells in the subgranular zone per unit length between the normal and low protein diet groups (Fig. 4).

On PND 77, only one TUNEL-positive apoptotic cell was detected in one animal in the normal protein diet group and there were no apoptotic cells in any of the animals in the low protein diet group (Fig. 4). There were no differences in the PCNA-positive cell ratio in the subgranular zone between the normal and low protein diet groups, similar to PND 21 (Fig. 4).

4. Discussion

In the present study, maternal protein restriction did not change the cellular distribution of immunoreactivity for Reelin, Calb-D-28K, or GAD67 in the dentate hilus on either PND 21 or PND 77. This suggests that the populations of GABAergic interneurons involving Reelin-synthesizing ones were not affected by maternal protein restriction through PND 77. This result is in contrast with the increases in GABAergic interneurons with immature phenotype in the hilus facilitating Reelin synthesis and in NeuN-

Table 3
Food consumption of offspring after maternal protein restriction during the second half of gestation and lactation.

	Males		Females	
	Normal protein20%[c]	Low protein10%[c]	Normal protein20%[c]	Low protein10%[c]
No. of offspring examined[a]	16	16	16	16
Food consumption (g/animal/day)				
PND 35	19.6 ± 1.7[b]	17.1 ± 0.7**	16.6 ± 1.7	15.5 ± 0.9
PND 42	27.3 ± 2.0	23.4 ± 1.2**	19.9 ± 1.6	19.1 ± 1.1
PND 49	30.4 ± 2.2	25.9 ± 1.4**	20.2 ± 1.2	19.0 ± 1.2
PND 56	32.3 ± 1.9	28.0 ± 1.6**	20.6 ± 1.3	19.1 ± 1.4*
PND 63	31.6 ± 2.0	27.9 ± 1.8**	20.9 ± 1.5	19.2 ± 1.4*
PND 70	32.1 ± 2.1	27.9 ± 2.0**	22.2 ± 1.9	20.3 ± 1.3*
PND 77	31.3 ± 2.1	27.4 ± 2.4**	20.7 ± 1.9	18.9 ± 1.5*
Food consumption (g/kg body weight/day)				
PND 35	141.7 ± 5.1	161.4 ± 9.0**	143.1 ± 8.3	161.1 ± 6.4**
PND 42	127.6 ± 3.4	137.8 ± 5.7**	122.9 ± 7.8	135.0 ± 4.7**
PND 49	105.8 ± 5.2	111.0 ± 4.0**	104.3 ± 6.6	109.1 ± 4.3*
PND 56	91.5 ± 4.6	96.3 ± 4.6**	94.6 ± 4.7	96.6 ± 3.4
PND 63	77.9 ± 3.9	82.3 ± 4.1**	86.5 ± 3.9	87.7 ± 5.4
PND 70	71.1 ± 4.0	73.6 ± 3.7	83.3 ± 4.6	84.8 ± 3.2
PND 77	63.8 ± 3.2	66.3 ± 3.5*	73.6 ± 4.0	75.3 ± 3.9

*, **Significantly different from the normal protein group by Student's or Aspin–Welch's *t*-test ($P < 0.05$; $P < 0.01$).
Abbreviation: PND, postnatal day.
[a] Identical two male and two female offspring per dam ($n = 8$/group) were used for food consumption measurement after weaning. Statistical analysis was performed using the litter as the experimental unit.
[b] Mean ± SD.
[c] Casein level.

Table 4
Organ weights of offspring after maternal protein restriction during the second half of gestation and lactation.

	Males		Females	
	Normal protein20%[c]	Low protein10%[c]	Normal protein20%[c]	Low protein10%[c]
PND 21				
No. of offspring examined[a]	10	10	10	10
Brain				
(g)	1.55 ± 0.05[b]	1.43 ± 0.03**	1.45 ± 0.05	1.34 ± 0.09**
(g/100 g BW)	2.38 ± 0.23	3.63 ± 0.40**	2.57 ± 0.19	3.98 ± 0.68**
Liver				
(g)	2.56 ± 0.39	1.67 ± 0.35**	2.36 ± 0.27	1.43 ± 0.41**
(g/100 g BW)	3.88 ± 0.23	4.16 ± 0.37*	4.15 ± 0.22	4.06 ± 0.43
PND 77				
No. of offspring examined[a]	10	10	10	10
Brain				
(g)	2.05 ± 0.06	2.01 ± 0.07	1.88 ± 0.05	1.85 ± 0.08
(g/100 g BW)	0.42 ± 0.02	0.48 ± 0.04**	0.66 ± 0.09	0.72 ± 0.06
Liver				
(g)	18.30 ± 2.58	15.16 ± 1.89**	10.07 ± 2.05	9.51 ± 1.46
(g/100 g BW)	3.68 ± 0.30	3.57 ± 0.18	3.48 ± 0.21	3.67 ± 0.24
Kidneys				
(g)	3.17 ± 0.50	2.83 ± 0.26*	2.07 ± 0.27	1.85 ± 0.15*
(g/100 g BW)	0.64 ± 0.07	0.67 ± 0.05	0.71 ± 0.04	0.73 ± 0.05
Testes				
(g)	3.58 ± 0.30	3.20 ± 0.47*	n.a	n.a
(g/100 g BW)	0.72 ± 0.05	0.76 ± 0.09	n.a.	n.a.
Ovaries				
(mg)	n.a.	n.a	97.3 ± 17.6	83.9 ± 9.9
(mg/100 g BW)	n.a.	n.a.	33.9 ± 4.3	32.8 ± 5.1

*, **Significantly different from the normal protein group by Student's or Aspin–Welch's *t*-test ($P < 0.05$; $P < 0.01$).
Abbreviations: BW, body weight; PND, postnatal day.
[a] One or two offspring of each sex per dam ($n = 8$/group) were subjected to autopsy and following organ weight measurement at each time point. Statistical analysis was performed using the litter as the experimental unit, and mean values were estimated as a litter value when two offspring were examined from the same dam.
[b] Mean ± SD; n.a.: not applicable.
[c] Casein level.

positive postmitotic neurons that we observed after developmental hypothyroidism and that were sustained through PND 77, which is suggestive of a mature population of GABAergic interneurons [15]. We observed neither an increase in NeuN-positive neurons in the hilus nor changes in cell proliferation or apoptosis in the subgranular zone in offspring of any age as a result of maternal protein restriction. The latter is in contrast with the increased apoptosis and decreased proliferation observed on weaning after developmental hypothyroidism, which is suggestive of impaired neurogenesis [15]. We also observed no changes in the distribution of hilar FoxG1-expressing cells after maternal protein restriction. Considering the role of FoxG1 in the regulation of neurogenesis in the postnatal hippocampus [24], and the lack of alterations in apoptosis and proliferation in the subgranular zone, maternal protein restriction may not affect postnatal neurogenesis of the dentate gyrus, reflected by an unchanged distribution of GABAergic interneurons.

Developmental hypothyroidism results in systemic growth retardation of the offspring in rats [10]. We have detected a similar effect of developmental exposure to anti-thyroid agents in rats, in which treatment of dams with 12 ppm PTU and 200 ppm methimazole (MMI) in the drinking water from GD 10 to weaning induced apparent and equivalent effects on changes in serum thyroid-related hormones in the offspring at weaning [16]. Body weights of the offspring in the hypothyroid cases were 64.2–68.8% of the non-treated group at weaning (Table 6). In the present study, a similar magnitude of offspring body weight reduction was observed after maternal protein restriction, with values being 65.5–65.8% of those in the normal protein group (Table 6). In our previous study, developmental hypothyroidism caused only a weak reduction in the absolute brain weights on weaning, with values after treatment with 12 ppm PTU and 200 ppm MMI being 94.5–97.9% of untreated controls (Table 6). However, maternal protein restriction was shown to decrease offspring brain weights [27,28], and in the present study we also observed greater reductions in absolute brain weights (91.7–92.9%) than in the developmental hypothyroidism study (Table 6). We also observed an increase in external granular cells in the cerebellar cortex on weaning after maternal protein restriction, which is suggestive of a delay in brain growth caused by systemic growth retardation. Thus, delayed brain growth due to systemic growth retardation does not influence populations of Reelin-synthesizing GABAergic interneurons and neurogenesis at weaning. These results strongly suggest that developmental hypothyroidism-induced brain changes observed at weaning in our previous study were solely caused by insufficient thyroid hormone signaling in the developing brain, and that delayed brain growth secondary to systemic growth retardation induced by hypothyroidism was minimal and unrelated to the observed neuronal changes.

In our previous study [16], we also observed lower body weights sustained through PND 77 after developmental exposure to anti-thyroid agents, with values after treatment with 12 ppm PTU or

Table 5
Histopathological examination of the cerebellum of male offspring at PND 21.

	Normal protein 20%[c]	Low protein 10%[c]
No. of offspring examined[a]	10	10
Cerebellum		
Increase of external granular cells (±/+)[b]	1(1/0)	5(3/2)*

*Significantly different from the normal protein group by Mann–Whitney's *U*-test ($P < 0.05$).
[a] Statistical analysis was performed using the individual animal as the experimental unit.
[b] Grade of change: (±), minimal: (+), slight.
[c] Casein level.

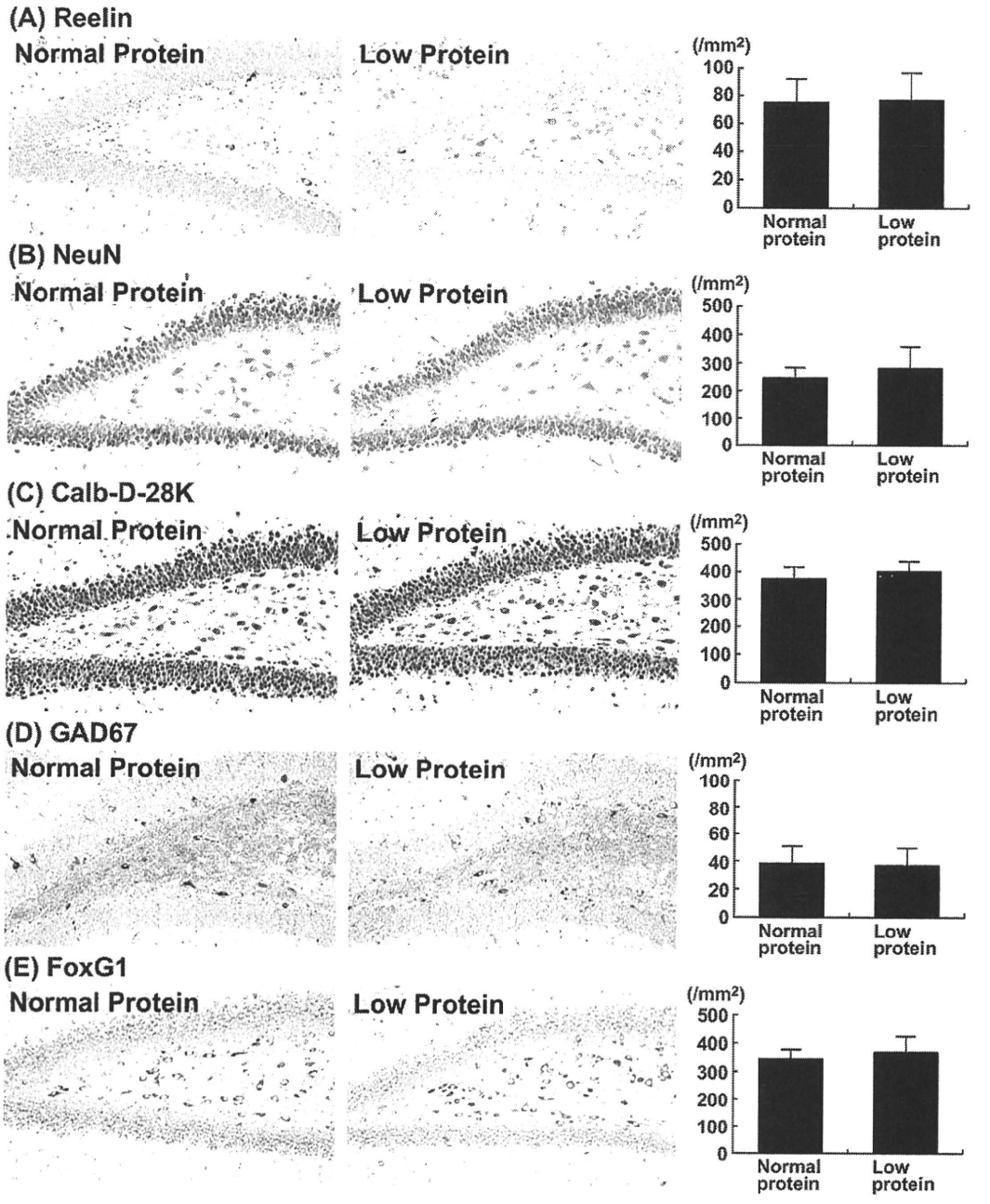

Fig. 2. Distribution of immunoreactive cells for Reelin, NeuN, Calb-D-28K, GAD67 and FoxG1 in the hilus of the hippocampal dentate gyrus in male offspring at PND 21 after maternal protein restriction from GD 10 to PND 21. All identical 10 male offspring from 8 dams (one or two animals per dam) were subjected to immunohistochemical analyses in each group. Statistical analysis was performed using the litter as the experimental unit, and litter mean values were subjected to analysis on two offspring samples from the same dam. (A) Reelin. (B) NeuN. (C) Calb-D-28K. (D) GAD67. (E) FoxG1. Representative image from the normal protein diet group (left) and from the low protein diet group (right). Magnification, 100× The graphs show the number of immunoreactive cells for each antigen/unit area (mm^2) of the hilus of the bilateral hemispheres at PND 21.

200 ppm MMI being 73.5–87.9% of untreated controls on PND 77 (Table 6). Maternal protein restriction during pregnancy and lactation causes a similar suppression of body growth sustained until the adult stage [29–31]. In the present study we observed a similar suppression in both sexes, with values in the low protein diet offspring being 84.0–89.3% of the normal protein diet offspring on PND 77 (Table 6). Interestingly, offspring from dams that were energy-restricted during lactation showed growth retardation at weaning but higher body weights at the adult stage than the control animals [31]. Although the mechanism is not clear, maternal protein restriction and developmental hypothyroidism may suppress body growth of the offspring until the adult stage by similar mechanisms. Male offspring in the hypothyroidism study showed apparent reductions in absolute brain weights on PND 77 after treatment with 12 ppm PTU or 200 ppm MMI (Table 6). This result is in contrast with the recovery in absolute weight on PND 77 after maternal protein restriction in the present study. White matter hypoplasia of the brain as a result of developmental hypothy-

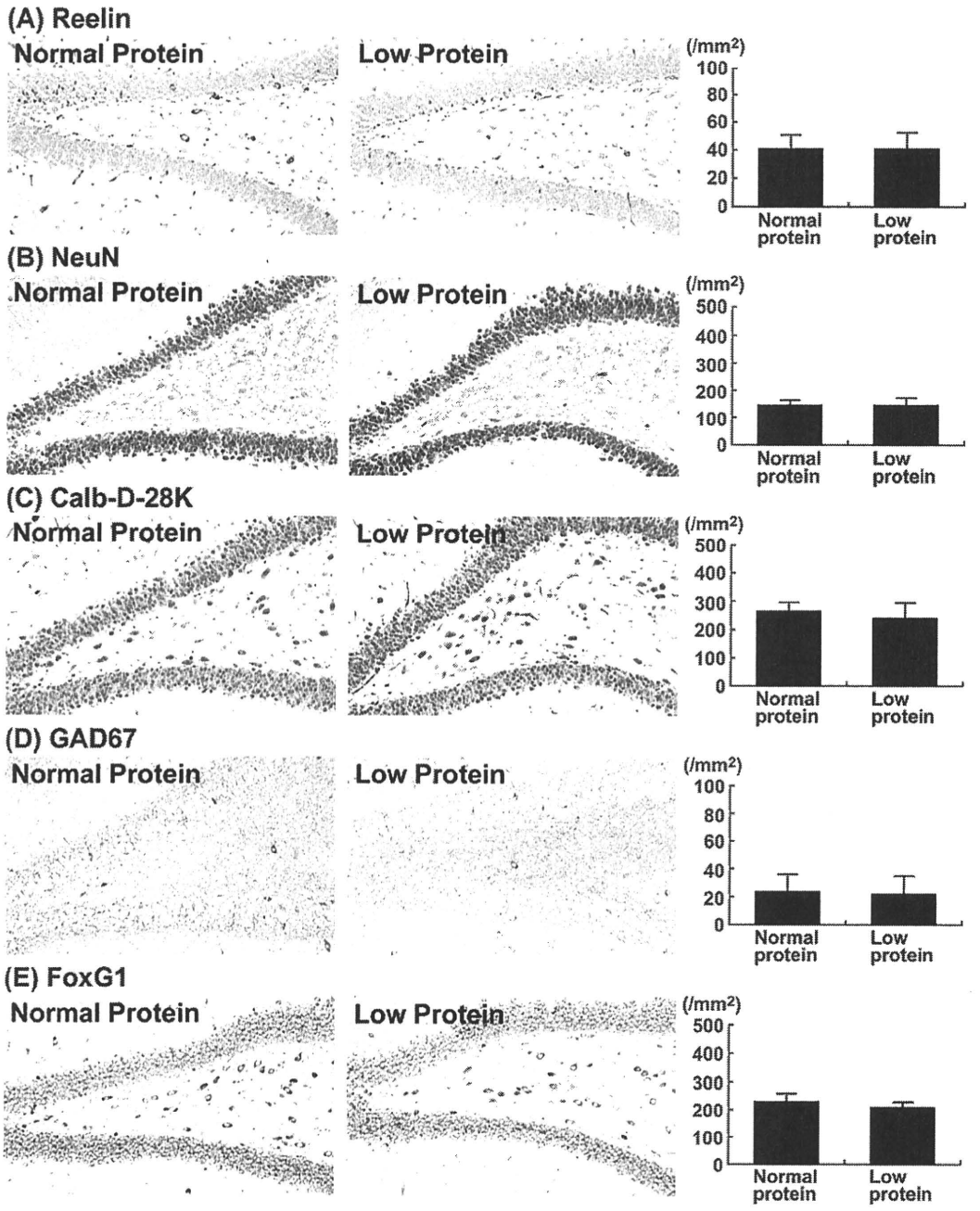

Fig. 3. Distribution of immunoreactive cells for Reelin, NeuN, Calb-D-28K, GAD67 and FoxG1 in the hilus of the hippocampal dentate gyrus in male offspring at PND 77 after maternal protein restriction from GD 10 to PND 21. All identical 10 male offspring from 8 dams (one or two animals per dam) were subjected to immunohistochemical analyses in each group. Statistical analysis was performed using the litter as the experimental unit, and litter mean values were subjected to analysis on two offspring samples from the same dam. (A) Reelin. (B) NeuN. (C) Calb-D-28K. (D) GAD67. (E) FoxG1. Representative image from the normal protein diet group (left) and from the low protein diet group (right). Magnification, 100×. The graphs show the number of immunoreactive cells for each antigen/unit area (mm^2) of the hilus of the bilateral hemispheres at PND 77.

roidism rather than delayed brain growth may be responsible for the reduction in absolute brain weight in the hypothyroidism cases [13,16]. These results suggest that the sustained systemic growth retardation allows recovery of brain growth through PND 77.

Developmental hypothyroidism resulted in a sustained increase in Reelin-synthesizing GABAergic interneurons at the later stage on PND 77 with increased population suggestive of immature phenotype [15]. This is in contrast with the unaffected distribution of GABAergic interneurons through PND 77 by maternal protein restriction. These results suggest that the sustained systemic growth retardation does not influence Reelin-synthesizing interneurons through PND 77. Maternal protein restriction during lactation results in elevation of serum triiodothyronine (T_3) levels due to an increase in thyroidal T_3 production in dams, and in continued higher serum concentrations of T_3 and thyroxine suggestive

Table 6
Comparison of body and brain weight data between the maternal protein restriction study and developmental hypothyroidism study.

	Maternal protein restriction	Developmental hypothyroidism[a]
Treatment	Fed diet with normal (20% casein) or low (10% casein) protein concentration between GD 10 and PND 21	Given PTU at 3 or 12 ppm or MMI at 200 ppm in the drinking water between GD 10 and PND 20
Weaning[b]		
Body weight		
Males	Low protein diet: 65.8%[c,**]	3 ppm PTU: 89.7%[d] 12 ppm PTU: 68.8%** 200 ppm MMI: 67.2%**
Females	Low protein diet: 65.5%**	3 ppm PTU: 86.3%** 12 ppm PTU: 65.0%** 200 ppm MMI: 64.2%**
Absolute brain weight		
Males	Low protein diet: 92.9%**	3 ppm PTU: 100.7% 12 ppm PTU: 97.9% 200 ppm MMI: 95.9%
Females	Low protein diet: 91.7%**	3 ppm PTU: 98.6% 12 ppm PTU: 95.2% 200 ppm MMI: 94.5%*
PND 77		
Body weight		
Males	Low protein diet: 84.0%**	3 ppm PTU: 99.7% 12 ppm PTU: 73.5%** 200 ppm MMI: 76.8%**
Females	Low protein diet: 89.3%*	3 ppm PTU: 87.9% 12 ppm PTU: 84.0%* 200 ppm MMI: 87.9%*
Absolute brain weight		
Males	Low protein diet: 98.5%	3 ppm PTU: 100.0% 12 ppm PTU: 90.5%** 200 ppm MMI: 92.4%**
Females	Low protein diet: 97.9%	3 ppm PTU: 101.6% 12 ppm PTU: 94.3% 200 ppm MMI: 96.9%

Abbreviations: GD, gestational day; MMI, methimazole; PND, postnatal day; PTU, 6-propyl-2-thiouracil.

[a] Published by Shibutani et al. [16].

[b] Offspring were weaned at PND 21 in the maternal protein restriction study and PND 20 in the developmental hypothyroidism study.

[c] Values were % ratios of the normal protein group with asterisks showing statistically significant difference by Student's or Aspin–Welch's *t*-test (**$P < 0.01$).

[d] Values were % ratios of the untreated group with asterisks showing statistically significant difference by Dunnett's test or Dunnett-type rank-sum test (*$P < 0.05$; **$P < 0.01$).

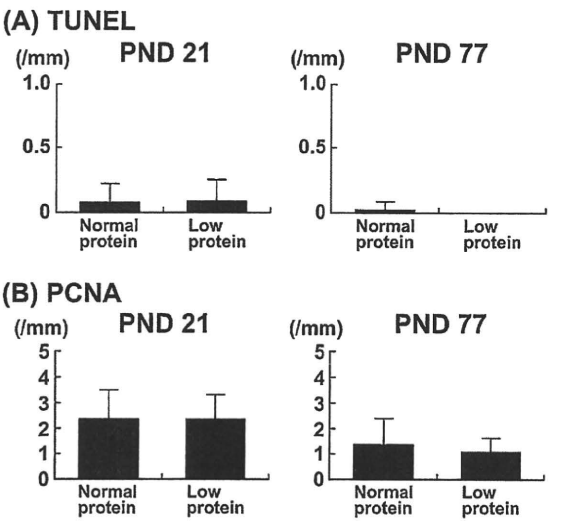

Fig. 4. Distribution of apoptotic cells and proliferating cells in the dentate subgranular zone of male offspring at both PND 21 and PND 77 after maternal protein restriction from GD 10 to PND 21. All identical male offspring (10 animals/group) as used in the immunohistochemical analyses on Reelin, NeuN, Calb-D-28K, GAD67 and FoxG1 at each time point were subjected to TUNEL-assay and PCNA-immunohistochemistry. Statistical analysis was performed using the litter as the experimental unit, and litter mean values were subjected to analysis on two offspring samples from the same dam. (A) Number of TUNEL-positive apoptotic cells/unit length (mm) of the subgranular zone of bilateral hemispheres at PND 21 and PND 77. (B) Number of PCNA-positive cells/unit length (mm) of the subgranular zone of bilateral hemispheres at PND 21 and PND 77.

of hyperthyroidism in the adult offspring [32,33]. Similar results were observed after maternal protein restriction during gestation and lactation as applied in the present study [34]. This observation is in contrast with the sustained but mild suppression of serum T_3 levels on PND 77 after developmental hypothyroidism in our previous study [16].

5. Conclusions

Maternal protein restriction resulted in systemic growth retardation sustained through PND 77 and retarded brain growth at weaning. However, it did not affect the distribution of Reelin-expressing GABAergic interneurons in the dentate hilus and postnatal neurogenesis in the subgranular zone through PND 77. These results suggest that systemic growth retardation accompanied by developmental hypothyroidism does not influence the impaired neuronal development caused by an insufficiency in thyroid hormone signaling in the brain. Because sustained increases in immature GABAergic interneurons synthesizing Reelin in the hilus could be a sign of a compensatory regulation for impaired neurogenesis and mismigration during neuronal development [15], monitoring of Reelin-expressing interneurons may provide a valuable tool for the detection of developmental neurotoxicants that can affect neurogenesis and migration. Importantly, Reelin-expressing immature cells are not affected by systemic growth retardation caused by systemic toxicity of dams and/or offspring.